



## **Long-term optimal capacity expansion planning for an operating off-grid PV mini-grid in rural Africa under different demand evolution scenarios**

Downloaded from: <https://research.chalmers.se>, 2024-04-18 19:09 UTC

Citation for the original published paper (version of record):

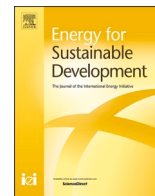
Wassie, Y., Ahlgren, E. (2023). Long-term optimal capacity expansion planning for an operating off-grid PV mini-grid in rural Africa under different demand evolution scenarios. *Energy for Sustainable Development*, 76. <http://dx.doi.org/10.1016/j.esd.2023.101305>

N.B. When citing this work, cite the original published paper.



Contents lists available at ScienceDirect

# Energy for Sustainable Development

journal homepage: [www.journals.elsevier.com/energy-for-sustainable-development](http://www.journals.elsevier.com/energy-for-sustainable-development)

## Long-term optimal capacity expansion planning for an operating off-grid PV mini-grid in rural Africa under different demand evolution scenarios

Yibeltal T. Wassie, Erik O. Ahlgren\*

Chalmers University of Technology, Department of Space, Earth, and Environment, Division of Energy Technology, SE-412 96 Gothenburg, Sweden

### ARTICLE INFO

#### Keywords:

PV mini-grids  
Capacity expansion  
Multi-year optimization  
Cost-effectiveness  
Reliability  
Unmet load

### ABSTRACT

Using real-time load data and HOMER Pro's 'multi-year' optimization tool, this paper investigates the long-term cost optimal capacity expansion planning (CEP) for an overloaded photovoltaic (PV) mini-grid (MG) with storage batteries in off-grid rural Ethiopia over a 20-year planning horizon. Three distinct annual energy demand growth scenarios were considered: 0 % (fulfils the minimum load requirement), 5 %, and a 15 % from productive users only. In all scenarios, the generation mix consists of only solar energy and the maximum allowable capacity shortage (MACS) is limited to 10 %. The findings reveal that, in all scenarios, the largest capacity expansion is performed on the battery and PV systems, covering up to 73 % and 35 % of the total expansion costs, respectively. The annual unmet load fraction of the expanded MG system ranges from 5.9 % in scenario-3 to 9.4 % in scenario-1, and the cost of electricity (LCOE) ranges from \$0.404/kWh in scenario-3 to \$0.887/kWh in scenario-1. The results indicate that the scenario-3 expansion path is comparatively cost-effective and has the highest reliability; but it still falls short of fully satisfying the required load demand and is not financially viable. Surprisingly, increasing the reliability of the scenario-3 capacity expansion from 94 % to 100 % raises the MG's Net Present Cost by 37 %. The sensitivity analysis shows that the MACS, ambient temperature, and battery's depth of discharge significantly affect the cost and performance of the capacity expansion. The study demonstrates (a) there are significant trade-offs between minimizing MG expansion costs and maximizing reliability levels; (b) capacity expansion based solely on cost-minimization without considering key constraints and uncertainties (demand, cost, PV, and battery degradations) may not provide a practical and robust solution to severe reliability issues, (c) capacity expansion that supports demand from productive users increases the cost-effectiveness and bankability of isolated MGs.

### Introduction

The pursuit of sustainable development requires a reliable and modern energy supply. As such, distributed Energy Systems (DES), such as Solar Photovoltaic (PV) mini-grids and mini-hydro power plants, are becoming increasingly important for improving access to electricity and fostering development, especially in remote areas in developing countries (IEA et al., 2022). In sub-Saharan Africa (SSA) alone, over 3000 mini-grids (MGs) have been installed by 2023 (World Bank, 2023). The majority of these are powered either by solar or hydro with battery energy storage system (BESS) and backup diesel generators (DG) (ESMAP, 2022; Fioriti et al., 2018). Nevertheless, a growing body of research shows that a significant number of the MGs deployed in off-grid areas of developing countries are experiencing serious reliability<sup>1</sup> issues

(Zebra et al., 2021; Numminen & Lund, 2019; Boruah, 2020), which, in most cases, arise from generation capacity shortages relative to the demand (Wang & Perera, 2019; Wassie & Ahlgren, 2023a; Moner-Girona et al., 2018). At the root of the capacity shortage problem lies inaccurate initial demand assessments, and subsequent under-sizing of the MG systems (Dawood et al., 2020; Louie & Dauenhauer, 2016; Lorenzoni et al., 2020). Another major drawback is that many MGs are designed using static and artificial load profiles, assuming that the present consumption levels of customers reflect their future energy needs. In essence, the dynamic nature of energy demand over time and its implications for MG sizing are overlooked (Allee et al., 2021; Khatib et al., 2013).

In practice, however, many rural households (HHs) and businesses connected to off-grid MGs in developing countries experience protracted power outages and unreliable electricity service within a short period of

\* Corresponding author.

E-mail addresses: [tebikew@chalmers.se](mailto:tebikew@chalmers.se) (Y.T. Wassie), [erik.ahlgren@chalmers.se](mailto:erik.ahlgren@chalmers.se) (E.O. Ahlgren).

<sup>1</sup> Throughout this paper reliability is defined in terms of adequacy, i.e., the ability of the mini-grid system to provide customers with electricity adequate to satisfy their requirements with minimum power interruptions (McCarthy et al., 2007).

<https://doi.org/10.1016/j.esd.2023.101305>

Received 13 July 2023; Received in revised form 22 August 2023; Accepted 25 August 2023

Available online 6 September 2023

0973-0826/© 2023 The Author(s). Published by Elsevier Inc. on behalf of International Energy Initiative. This is an open access article under the CC BY license (<http://creativecommons.org/licenses/by/4.0/>).

Abbreviations and acronyms	
AC	Alternating Current
BESS	Battery Energy Storage System
$C_C$	Capital Cost
CEP	Capacity Expansion Planning
$C_{O\&M}$	Operation and Maintenance Costs
CRF	Capital Recovery Factor
DC	Direct Current
DES	Distributed Energy System
DG	Diesel Generator
DOD	Depth of Discharge
DPP	Discounted Payback Period
DSM	Demand-side Management
DSS	Degree of Self-Sufficiency
EEU	Ethiopian Electric Utility
$E_{unmet}$	Total Annual Unmet Load
$f_{CS}$	Capacity Shortage Fraction
$f_{unmet}$	Unmet Load Fraction
HH	Household
HOMER	Hybrid Optimization of Multiple Energy Resources
$K_p$	PV module's Temperature Coefficient of Power
LCC	Life Cycle Cost
LCOE	Levelized Cost of Energy
MACS	Maximum Annual Capacity Shortage
MG	Mini-grid
MI	Multiple Imputations Method
MPPT	Maximum Power Point Tracker
NPC	Net Present Cost
$O_c$	Operating Cost
O&M	Operation and Maintenance
PMM	Predictive-mean Matching
PV	Photovoltaic
RES	Renewable Energy Sources
$R_C$	Replacement Cost
RF	Renewable Fraction
SI	Solar Irradiance
ROI	Return on Investment
SMEs	Small and Medium Enterprises
SOC	State of Charge
SSA	Sub-Saharan Africa
STC	Standard Test Conditions
$T_a$	Ambient Temperature
TNPC	Total Net Present Cost

installation of the MGs, mainly due to capacity shortfalls (Amara et al., 2021; Shyu, 2013; Waqar et al., 2015). In Omorate (southern Ethiopia), recent studies (Wassie & Ahlgren, 2023a; Wassie & Ahlgren, 2023b) based on real-time electricity generation and load data show that the daily average power supplied by the PV MG (1100 kWh) was unable to fully meet the daily load demand (1808 kWh). As a result, the load is completely shed off for 12–13 h each day to match the demand with the output. The same studies indicate that the capacity deficit was mainly attributable to under-sizing of the battery bank and PV array, exacerbated by large PV capture losses and high ambient temperatures in the area. Given the size of the daily unmet load, conventional demand-side management (DSM) strategies such as Load Shifting, or Time-of-Use based pricing are unlikely to resolve the reliability issues caused by such capacity shortages.

The main strategy for addressing severe reliability issues and frequent power outages brought on by capacity shortages in power systems is to expand the existing generation capacity. Nonetheless, capacity expansion requires significant investment, which raises the critical question of how to do so in the most cost-effective manner. Which technology mixes and component sizes provide the most cost-optimal capacity? How should the reinforced system be operated to maximize reliability in the face of uncertainties and constraints? Answering these questions and determining the most optimal generation (and storage) capacity necessitates solving an economic capacity expansion planning (CEP) problem, subject to key operational constraints and uncertainties.

Research on renewable-based off-grid MGs has thus far been dominated by techno-economic feasibility analyses (Dawood et al., 2020; Khatib et al., 2013; Amara et al., 2021; Gabra et al., 2019), while capacity expansion planning of these technologies has received little attention. The summary of recent studies pertinent to CEP of MGs (Table 1), shows that many of the few studies conducted were concentrated either on grid-tied MGs (Mohseni et al., 2020; Sayani et al., 2022) or on developing new CEP methodologies and optimization algorithms using synthesized load profiles (Waqar et al., 2015; Wang et al., 2017). A handful of studies have been conducted on optimal CEP for off-grid MGs based on measured load data (Hartvigsson et al., 2018; Groissböck & Gusmão, 2017). Almost all of these studies relied on single-year optimization approaches using constant or repetitive load profiles and extrapolating the results to the MG life-cycle. The single objective criteria of the CEP in most studies was cost minimization. Furthermore,

the simulations were based on manufacturer-specified equipment performance data under standard test conditions (STC) rather than real-world outdoor performance of the equipment.

Consequently, these studies hardly capture effects of demand evolution over time, particularly from productive<sup>2</sup> users, effects of local climatic conditions, and uncertainties in input variables on the technical and economic performances of the expanded system. Failure to take into account these critical factors in the CEP could not only result in recurrence of reliability issues but also jeopardize the return on investment of capacity expansions (Lorenzoni et al., 2020).

This study builds on a recent performance analysis on a 375 kWp operating PV-battery MG system (Wassie & Ahlgren, 2023a). The main objectives of the study are to determine the long-term optimal generation capacity additions that satisfy the required load, reliability, and other system constraints with the lowest cost under varying demand evolution scenarios, and to investigate trade-offs between its technical and economic performances.

The paper specifically addresses the following research questions:

- What component sizes and capacity additions provide the most cost-effective solution to meet the load demand, reliability, and other system constraints in each scenario?
- How does the techno-economic performance and robustness of the capacity expansion solution change over time under different energy demand growth scenarios?
- What are the trade-offs between capacity expansion cost and reliability levels in the different expansion paths, and what do these trade-offs imply for optimal CEP of off-grid MGs?
- How do operational constraints and uncertainties in input variables affect the technical and economic performances of the reinforced MG system?

This study is innovative in many respects:

<sup>2</sup> Productive use, in this paper, refers to the use of electricity primarily for businesses or income generation purposes.

**Table 1**  
Summary of selected renewable based mini-grid capacity expansion studies.

Ref.	System design	Off-grid	Load data source or forecasting method	Optimization tool/method	Findings and contributions
18	Micro-hydro/PV/Biomass/BESS/DG	X	Based on a grid with capacity shortage of around 29.3 %/year.	Stochastic optimization approach	Not accounting for uncertainties leads to underestimation of the total net present cost (NPC) of capacity additions by 23 %.
22	Wind/PV/BESS	X	Forecasted demand based on current load.	HOMER	The existing tariff rate can well recover the cost of the capacity expansion.
23	PV/BESS	X	Adaptive demand forecasted based on energy use surveys.	CLOVER	Cost-saving of up to 12 % can be realized when MGs are expanded in several stages as opposed to in a single phase.
24	PV/Wind/BESS/DG	✓	Forecasted load based on demand scenarios.	A Tri-level expansion planning framework	Using controllable loads (loads which can be switched off and on as required), when renewables are not sufficient, increases the yearly profit by 25 %.
25	Hydro/PV/Wind/BESS/DG	✓	Forecasted demand based on actual static load profiles.	DER-CAM	The cost-minimized expansion has poor financial return due to high investment costs. The diesel-only expansion plan suffers from high operational costs.
26	PV/Wind/Concentrated solar power/Open-cycle gas turbine	✓	Actual hourly load profiles for one year with assumed different renewable energy penetration levels.	GNU-Octave	Adding renewable energy source capacity is more economical for systems with peak load growth rates <5 % while systems with peak load growth rates >5 % still need to incorporate fossil fuels (gas).

- First, the CEP<sup>3</sup> utilizes real-time metered initial load data; thus, it minimizes the adverse effects of initial load assessment errors.
- Second, the study uses a multi-year dynamic optimization approach incorporating year-by-year changes in energy demand and other input variables instead of a single-year simulation using a constant or repetitive load profile.
- Third, besides the cost-minimization objective, the CEP considers maximizing power supply reliability from a 100 % renewable fraction (RF) in the generation mix.
- Fourth, the optimization accounts for the effects of ambient temperature, and PV and battery performance degradations over time, resulting in a more robust and reliable CEP model.

The CEP is performed using the HOMER<sup>4</sup> Pro optimization tool over a 20-year planning period. Three distinct annual energy demand growth scenarios are considered: 0 % (fulfils the minimum required load), 5 %, and a 15 % for productive users only. In all three scenarios, a 100 % solar energy resource and a maximum annual allowable capacity shortage (MACS<sup>5</sup>) of 10 % are imposed.

## Methodology

### Description of the existing MG system

#### Location

The MG system investigated in this work is located in a remote small town named Omorate, in southern Ethiopia. It was selected due to its significant capacity shortage (Wassie & Ahlgren, 2023a), availability of operational data, its location in a hot semi-arid tropical climate, and the fact that it is among the first off-grid PV MGs installed for rural electrification in Ethiopia. Omorate lies between 4°80'16"N Latitude and 36°3'29' E Longitude with an average elevation of 368 m.a.s.l. The mean

annual temperature is 29.2 °C. The location map and infrastructure of the mini-grid is presented in Appendixes A and B, respectively. According to information obtained from the EEU<sup>6</sup>, the MG began generating power in late April 2021. By December 2021, a total of 443 customers (301 HHs, 112 small-businesses, and 30 institutions) were connected to the MG. As of December 2021, approx. 350 HHs (out of the over 770 total HHs) were waiting to be connected to the MG.

#### Current installed capacity and configuration of the existing MG system

The MG is alternating current (AC)-coupled with a total installed capacity of 375kWp. It consists of six system components: PV panels, converters (solar direct current (DC) to AC inverters and battery DC/AC converters), maximum power point trackers (MPPTs), BESS comprised of five LiFePO<sub>4</sub> battery packs with a total nominal storage capacity of 600 kWh, a DG with 100 kW power, a distribution board, and loads. The PV array comprises 1210 series-connected mono-crystalline modules from Jinko. Each module has a rated power of 310 Wp and efficiency of 18.94 % at STC. The modules are assembled into 9 strings in two parallel rows. Each string is connected to one converter with a maximum output power of 50 kWp. Each converter has 6 MPPTs and all the modules in each string are mounted on racks fixed on the ground, facing towards south at 15° tilt.

Although the MG has a backup DG, it has not been used to generate power so far, except in a few exceptional circumstances, due to the high price (more than \$1.8/liter) and inaccessibility of diesel fuel in the area. According to (Asress et al., 2013), wind resources in the area are low. Therefore, solar energy is the only energy resource considered for power generation in the CEP. All system components, except the DG, are included in the CEP. A schematic illustration of the MG is presented in Fig. 1. Additionally, Appendix C provides detailed technical specification of the existing MG system.

#### Input data and data sources

##### Meteorological data

Data on daily solar irradiation (SI), ambient temperature (Ta) and clearness index at the MG site were obtained from NASA's global energy resource database (NASA, 2023). The data covers 20 year-period (2001

<sup>3</sup> The technologies and costs considered in this study are restricted to only the energy production system (PV, Converters and the BESS). It does not include the distribution and end-use systems, or other related costs.

<sup>4</sup> The Hybrid Optimization of Multiple Energy Resources (HOMER) pro is an optimization software widely used to determine the optimal sizing of island micro-grids involving combinations of renewable and/or conventional energy resources. A detailed description of the software is available at <https://www.homerenergy.com/>.

<sup>5</sup> The MACS is the ratio of the maximum allowable amount of the total deficit that occurs between the required capacity and the actual capacity the system can supply to the total electric load (Mohseni et al., 2020).

<sup>6</sup> Ethiopian Electric Utility (EEU) is a state-owned utility company that manages power distribution and sales from all power plants in Ethiopia including off-grid mini-grids. In 2016/17, the EEU identified 250 rural small towns that are isolated from the national power grid and need to be electrified using PV/battery/diesel hybrid mini-grids. The Omorate MG is among the first twelve mini-grids installed in the country out of the 250 planned.

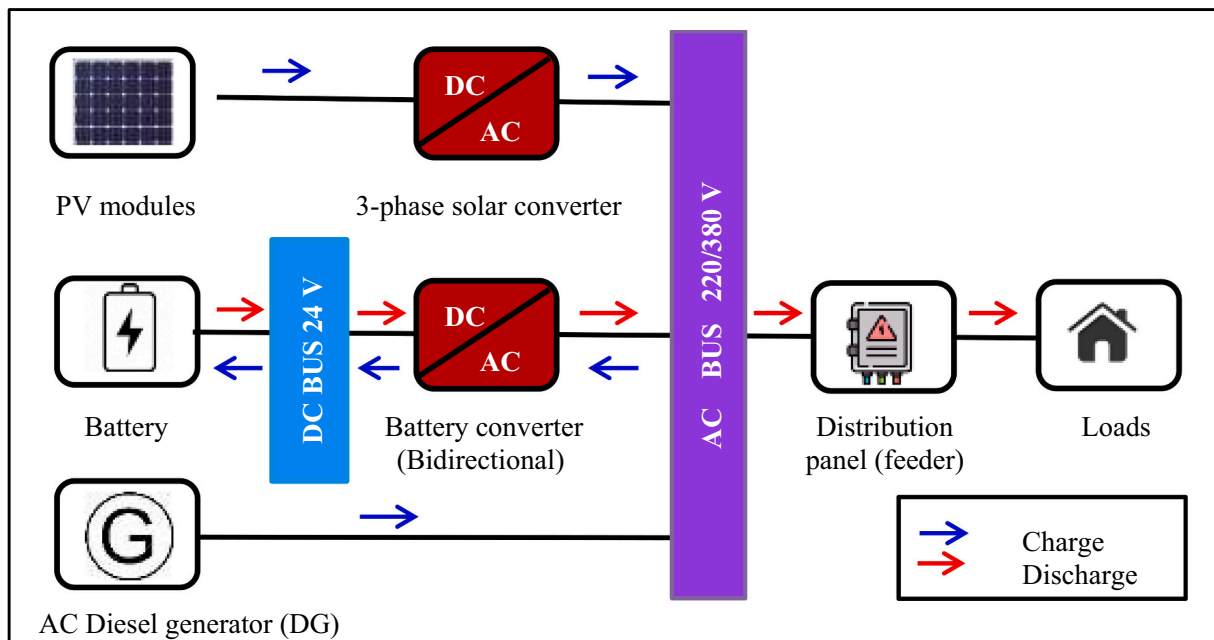


Fig. 1. Schematic illustration of the Omorate AC-coupled hybrid MG system.

through 2021). Fig. 2 presents monthly average solar irradiation and clearness<sup>7</sup> index of the site over the 20 years. According to Fig. 2, the site has abundant solar energy potential with a daily average irradiation of 6.01 kWh/m<sup>2</sup>/day, varying narrowly between 5.6 kWh/m<sup>2</sup>/day in July to 7.1 kWh/m<sup>2</sup>/day in January.

#### Daily primary load data and missing data imputation

This study is based on actual daily electrical load data drawn directly from the Energy Management and Control System of the MG over the first 20 months (610 days) of its operation. The daily load report contains detailed information on the hourly load P (kW) and its distribution patterns, among other things. Appendix D provides the daily load report for a typical weekday in December 2022. As mentioned earlier, the load is currently interrupted for about 13 h each day. This means that the observed electricity consumption is a suppressed one and does not reflect the true demand of the customers. In order to determine the optimal generation capacity, the unsuppressed load, the sum of the current suppressed load and the unmet load, must be calculated. This calls for imputing the missing load data during the load-shedding hours. Several methods are used in the power industry to impute missing load data including the nearest neighbor method, linear interpolation, etc. (Ruggles et al., 2020). However, since the missing load data points in this case are multiple and nonrandom; conventionally applied methods may not accurately predict the missing data values. According to (Seaman et al., 2012; White et al., 2011), a more suitable method that delivers more accurate estimates of multiple missing data when the quantitative variable is non-normally distributed is the Multiple Imputations (MI) method based on the predictive-mean matching (PMM) technique. Fig. 3 displays that the load data in the existing MG are nonrandom and non-normally distributed.

The MI method is embedded in many software packages in the form of 'Multiple Imputations by Chained Equations (MICE)'. In this study, the missing load data values, during the load-shedding hours were imputed using the MI method built in STATA version 16. The solid line

in Fig. 3 denotes the average actual uninterrupted daily load curve in May 2021 and the broken line denotes the unsuppressed daily load profile in December 2022 including the imputed loads. Accordingly, the unconstrained daily energy demand and hourly load data for each of the 365 days in 2022 were established. This daily electrical load dataset is then used as the minimum energy requirement of the current customers in the demand projection and CEP.

#### Unsuppressed annual electrical demand profile of different customers

With the unsuppressed daily load curves now established, the annual energy requirements and load profiles of the different customer groups is computed using the consumption data obtained from the EEU. The EEU dataset provides detailed information on the monthly metered consumption by customer type (sector) including the billing month, consumption charge, and tariff rates. According to this data, the average monthly energy delivered to all customers in 2022 was 32.4 MWh and the total energy delivered by the MG in 2022 was 388.8 MWh. Based on this annual consumption data by sector and the unsuppressed load curve in Fig. 3, it is calculated that the minimum energy requirement of the MG customers in 2022 was 638.8 MWh, of which 250MWh was unmet.

#### Adaptive demand growth scenarios definition

Three distinct demand growth scenarios are considered for the CEP. The three demand scenarios are established based on the following data, observations, and experiences. First, the population in the area is growing, and urbanization is expanding (Wassie & Ahlgren, 2023b). Second, new connections to the MG are suspended by the EEU due to generation capacity shortages. This has led to a rise in unauthorized connections to the MG (Wassie & Ahlgren, 2023b). Third, the data in Table 2 shows that about 40 % of the annual energy demand of customers is unserved by the current capacity. The same data reveals that productive users account for over 50 % of the total annual consumption. At the same time, new businesses are being opened. Fourth, given the remoteness of the town and the prohibitive cost of grid expansion, the main grid is not expected to compete with the MG, at least during the planning period. Further, an earlier study on an off-grid MG in Tanzania found a 15 to 25 % annual growth rate of electricity consumption over the course of 30 months (Hartvigsson et al., 2021). All these evidence and data point that, at least in the short to medium term, a substantial increase in the town's electricity demand is highly likely. Hence, the

<sup>7</sup> The **Clearness index** is a measure of atmosphere clearness. It is defined as the ratio of the solar irradiance reaching the earth's surface to the corresponding extraterrestrial solar irradiance at the top of the atmosphere (NASA, 2023).

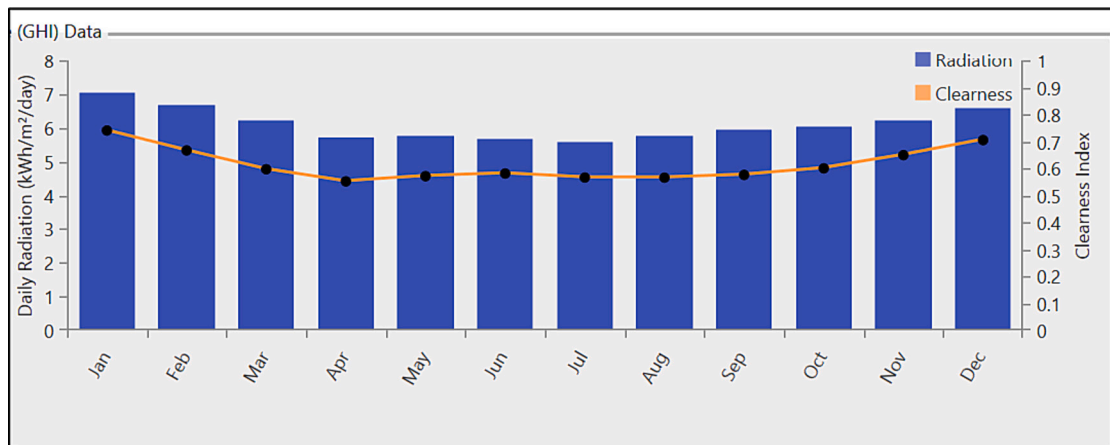


Fig. 2. Monthly average daily solar irradiation and clearness index at the MG site (NASA, 2023).

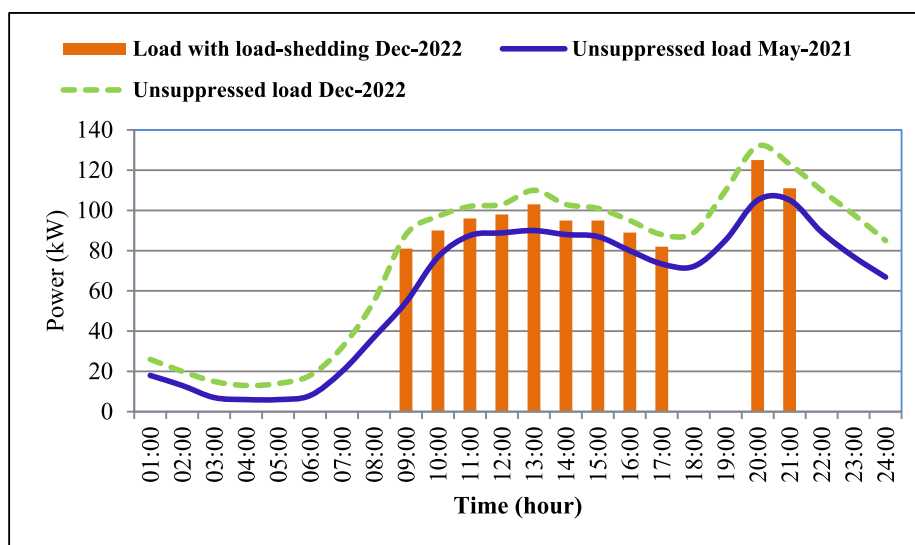


Fig. 3. Daily suppressed and the unsuppressed average load profiles of the existing MG in 2022.

Table 2

Annual suppressed and unsuppressed load profiles of customers by sector in 2022.

Sector	#	Current load (MWh/year)	% Load share	Unmet load (MWh/year)	Unsuppressed load (MWh/year)
Households	301	155.5	40.0	100.0	255.5
Productive/SMEs	112	197.1	50.7	126.7	323.8
Institutions	30	35.8	9.2	23.0	58.8
Streetlights	11	0.4	0.1	0.3	0.7
<b>Total</b>		<b>388.8</b>	<b>100</b>	<b>250</b>	<b>638.8</b>

demand growth scenarios for the long-term CEP must be adaptive and able to account for changes in the demand evolution trajectory that may result from the local population growth, urbanization, socio-economic development, and other drivers.

With these considerations, the three demand growth scenarios are defined as follows. Fig. 4 and Appendix E present the demand trend and the corresponding predicted demand data in MWh/year for each scenario over the 20-year planning horizon, respectively.

**Base case (BC) scenario:** assumes that, throughout the planning period, the constrained electricity consumption of the current

customers, which is on average 1065 kWh/day and 389 MWh/year, will continue unchanged. The BC scenario represents the MG’s current generation capacity.

**Scenario 1 (S1):** is defined as the minimum unsuppressed energy requirement of the current MG customers, which is estimated to be on average 1750 kWh/day and 639 MWh/year. It represents the minimum generation capacity required to satisfy the primary load of the current MG customers without allowing for future growth in demand.

**Scenario 2 (S2):** assumes a 5 % annual demand growth rate beginning with S1 (the minimum unsuppressed demand). This results in a mean daily and annual demand of 3039 kWh and 1109 MWh, respectively over the CEP period. Currently, at least 350 HHs are waiting for authorized MG connection from the EEU. Thus, S2 focuses on serving the additional demand from these 350 HHs and other new customers, as well as demand growth from new and existing customers.

**Scenario 3 (S3):** assumes a 15 % annual demand growth rate for productive users only, beginning with S1. This results in an average daily and annual demand of 4075 kWh and 1487 MWh, respectively. Table 2 displays that productive users consume >51 % of the annual energy supplied by the MG despite representing only 25 % of the total number of MG customers. Scenario-3, therefore, aims to fulfill a potentially large demand growth from existing and new productive users as well as to satisfy the power demand for cooking, welding, woodwork, and garage services, etc., that are presently not encouraged

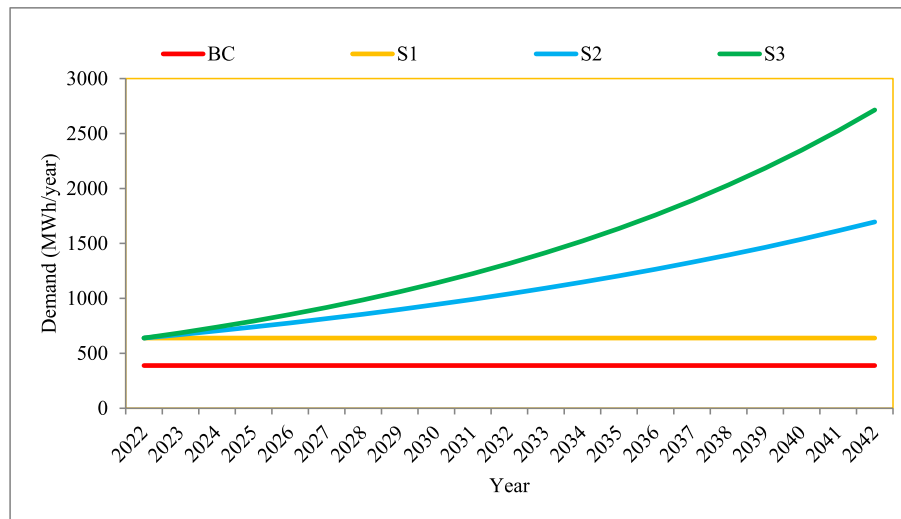


Fig. 4. Annual load demand growth scenarios considered for the capacity expansion.

by the EEU due to the serious capacity shortages.

*Cost break-down of the existing MG system*

The actual financial data on the initial capital costs ( $C_C$ ) of the MG system were obtained from the EEU and the project document signed between the EEU and the Guodian Nanjing Automation Co. Ltd. (the contractor). The annual operating and maintenance costs ( $C_{O\&M}$ ) were obtained from the EEU district and regional offices. The total initial  $C_C$  of the MG, excluding the DG, was US\$ 1.16 ml; of which the  $C_C$  of PV including the installation costs was \$800,000. The  $C_C$  of converters including MPPT controllers was \$141,828, and the  $C_C$  the BESS was \$216,769. The replacement cost ( $R_C$ ) of all system components was calculated assuming a 10 % drop in purchase price of each technology as per the recommendations of the contractor. The annual  $C_{O\&M}$  of the system was roughly \$20,400 in 2022. The nominal discount rate and inflation rate in Ethiopia in 2022 were 7 % and 25 %, respectively. Table 3 details the cost data per kWp capacity by component type.

**Modeling approach and evaluation parameters**

*Multi-year dynamic capacity optimization using HOMER Pro*

A multi-year, dynamic and forward-looking optimization approach is used for the CEP. A separate optimization is performed for each scenario using the HOMER Pro version 3.15 equipped with the ‘multi-year’ and ‘advanced storage’ modules. The major advantage of HOMER Pro with the multi-year module is that it allows the user to perform dynamic and robust optimization of the long-term operation of a MG system by specifying and incorporating expected changes and uncertainties in input variables that can occur over the MG’s life-cycle but cannot be

**Table 3**

Input cost data for each component (based on actual data obtained from the EEU).

System component	Capacity/ quantity	Lifetime (years)	Initial $C_C$	$R_C$	$C_{O\&M}$
Solar PV	1 kW	20	2133 (\$/kW)	1920 (\$/kW)	13.5 (\$/kW/year)
Converter	1 kW	10	315 (\$/kW)	284 (\$/kW)	4.30 (\$/kW/year)
Battery	1 (600 kWh)	10	\$216,769	\$195,092	\$13,402/year

captured by the traditional single-year simulation, which uses a static load and extrapolates the results to the MG’s lifetime. These changes and uncertainties can include annual increases in load,  $C_C$ ,  $C_{O\&M}$ , interest rates, and component degradations, etc. and can be input as percentages or multipliers. HOMER Pro achieves the multi-year dynamic optimization by running a year-by-year simulation, incorporating these changes. When applied in combination, the multi-year and advanced storage modules allow the user to model the effects of temperature on the battery lifespan and PV performance degradations, and the resultant effects on the PV output and system costs (Lambert, 2006). In doing so, it enables the modeler to draw important insights into the complexities and tradeoffs associated with long-term CEP of reliable and robust distributed solar MG systems at the lowest cost possible. Moreover, HOMER presents simulation results in a wide variety of tables and graphs that allow the user to compare feasible configurations and evaluate them on their economic and technical merits.

HOMER primarily performs three tasks: simulation, optimization, and sensitivity analysis. In the simulation process, it models input data and identifies all feasible system configurations, operating strategies, and combination of system components of specific sizes that satisfy the load and other constraints specified by the modeler (HOMER Energy, 2022; Lambert, 2006). After the simulation is complete, HOMER computes the NPC of each feasible system configuration. In the optimization stage, HOMER determines the most optimum system configurations based on the calculated NPC out of the many viable solutions identified in the simulation. It then sorts the optimum configurations from the lowest to the highest NPC. In the case of this study, the optimization results are used to determine the most optimal MG capacity in each scenario and calculate the additional capacity needed to meet the load. To control the battery’s operation and utilization of the power produced, the load following (LF<sup>8</sup>) dispatch strategy is used. The reason is that, the LF control strategy prioritizes the battery bank to be charged by the excess power produced by renewable sources, while the dispatchable energy sources such as the DGs and BESS will only generate power when the power output from the renewables does not meet the demand (HOMER Energy, 2022; Jufri et al., 2021). This makes the LF strategy best suited for the capacity optimization of the present MG system, which fully relies on solar energy. In the sensitivity analysis, a separate optimization for each specified value of a sensitivity variable is conducted. A sensitivity variable is a variable that can affect the technical

<sup>8</sup> A detailed description of the different dispatch strategies employed by HOMER Pro is given in (HOMER Energy, 2022; Jufri et al., 2021).

**Table 4**  
Optimization constraints and uncertainties.

Optimization constraints and uncertainties	Values	Source
Project life-cycle	20 years	Based on manufacturer
Maximum allowable annual capacity shortage	10 %	This paper
Nominal PV cell operating cell temperature	45 °C	Manufacturer
Minimum and maximum battery state of charge (SOC)	30 %, 90 %	Manufacturer
PV module's temperature coefficient of power ( $k_p$ )	-0.45 %/°C	(Dash & Gupta, 2015)
PV performance degradation per year	1.54 %/year	(Han et al., 2018)
Battery degradation per year	%/year	Determined by HOMER
Demand random variability (day-to-day)	10 %	(Wassie & Ahlgren, 2023a)
Increase in $C_c$ of components at the end of lifetime	-10 %	This paper
Annual increase in $C_{O\&M}$ by component	5 %/year	This paper

and economic performances of the expanded MG system and for which multiple values can be specified. Table 5 details the sensitivity variables used in this analysis that are chosen based on review of relevant literature (Wassie & Ahlgren, 2023a; Louie & Dauenhauer, 2016; Gabra et al., 2019; Hartvigsson et al., 2018).

*Optimization constraints, uncertainties, and sensitivity variables*

Given the objectives of the CEP, a set of operational constraints or criteria that must be met by the reinforced system are imposed. As indicated earlier, the MACS in this analysis, is allowed to vary between 0 % (the MG must serve 100 % of the load at all times) and 10 % (the MG must serve 90 % of the load at all times). The justification is that the existing MG capacity has an average annual unmet load fraction,  $f_{unmet}$ , of about 40 %, therefore the expanded system should reduce this unmet load significantly. Accounting for expected changes and uncertainties is another important factor for achieving a robust CEP. Table 4 presents the model constraints and anticipated year-by-year changes in input variables, based in part on evidence from prior studies in similar settings.

*Capacity expansion optimality assessment*

The optimality<sup>9</sup> of generation capacity expansion, in this study, is primarily measured in terms of two performance metrics: reliability of energy supply and average cost of electricity production.

*Energy supply assessment*

To assess the energy performance of the optimally expanded MG capacity, the total annual power generation, primary<sup>10</sup> load served, unmet load ( $E_{unmet}$ ), unmet load fraction ( $f_{unmet}$ ), capacity shortage fraction ( $f_{CS}$ ) as well as the battery bank's autonomy, storage depletion and energy losses are used. The  $E_{unmet}$  is the total amount of unmet electrical load that the system is unable to serve throughout the year (kWh/year), whereas the  $f_{unmet}$  is the proportion of the total annual electrical load that went unserved due to inadequate generation.

<sup>9</sup> In this study, the environmental aspects (CO<sub>2</sub> emissions reductions) of the optimal generation capacity expansions are not analyzed since the power generation mix does not involve diesel fuel or other fossil fuels.

<sup>10</sup> A primary load is an electric load that is given the highest priority in the system for demand fulfillment as opposed to a "deferrable load" that can be scheduled, stopped, or wait until surplus power is available. In PV-battery systems, the load associated with storage is normally referred to as "deferrable". Accordingly, in HOMER simulation, the resources always supply electricity to the primary load first, then go to the deferrable load.

**Table 5**  
Sensitivity variables.

Sensitivity variables	Values	Source
Maximum annual capacity shortage	0 %, 1 %, 2 %, 3 %, ...9 %, 10 %	This paper
Average ambient temperature (°C)	24, 26, 28, 30, 32, 42, 44, 48	(Wassie & Ahlgren, 2023a; Wassie & Ahlgren, 2023b)
Battery Depth of Discharge (DOD) (%)	10, 20, 30, 40, ...	This paper
Real interest rate	7 %, 8 %, 9 %, ..., 13 %, 14 %	This paper

*Economic performance assessment*

The total NPC, also called the life cycle cost (LCC), of a system is HOMER's primary metric, by which it ranks all system configurations in the optimization results. It represents the present value of all costs the system incurs over its working lifetime [including the  $C_c$  of system components,  $R_c$ ,  $C_{O\&M}$  and other costs,] minus the present value of all potential revenues the system earns over its lifetime (HOMER Energy, 2022). The TNPC is calculated by using Eq. (1) as:

$$TNPC = \frac{C_{ann.tot.}}{CRF(i, N)} \tag{1}$$

where  $C_{ann.tot.}$  is the total annualized cost, and  $CRF(i, N)$  is the capital recovery factor, which is the ratio used to calculate the present value of equal annual cash flows over the system's lifetime;  $i$  is the real discount rate and  $N$  is the lifetime in years.

$$C_{ann.tot.} = (CRF * Capital_{cost}) + O\&M_{cost} \tag{2}$$

$$CRF(i, N) = \frac{i(1+i)^N}{(1+i)^N - 1} \tag{3}$$

The LCOE is defined as the average cost per kWh of useful electricity produced by the MG (HOMER Energy, 2022). According to Brooks (2014) and Zhao et al. (2017), the LCOE metric is superior to NPC for comparing the economic performance of projects with significant differences in size since it has no restrictions on project scale. In contrast, the NPC is more useful for comparing the economic performance of similar-sized projects. Due to this, we have mainly relied on LCOE to assess the cost-effectiveness of the capacity expansion under the different demand scenarios. The higher the LCOE, the lower the economic optimality of the capacity expansion. LCOE is calculated using Eq. (4) (Lambert, 2006).

$$LCOE = \frac{\sum_{t=1}^N \frac{I_t + O\&M_t}{(1+i)^t}}{\sum_{t=1}^N \frac{E_t}{(1+i)^t}} \tag{4}$$

where  $I_t$  is the initial investment cost in year  $t$ ,  $O\&M_t$  is the operations and maintenance cost in year  $t$ ,  $E_t$  is the electricity produced in year  $t$ ,  $i$  is the discount rate, and  $N$  is MG's life in years.

**Results**

*Optimization results*

The multi-year optimization results, shown in Table 6, reveal significant differences in component sizes of the optimal MG system across the three scenarios. Noticeably, the PV array, converter, and battery capacities of the system in S3 are much larger than those in S1 and S2. When compared to the BC, the PV and battery sizes of the system under S3 are roughly three or more times larger. Similarly, the total net present cost (TNPC) is highest for the MG in S3 and lowest in S1. As stated in the objective, this work is not about comparing the three scenarios per se, but about the optimal capacity expansion of an operating MG under different demand growth scenarios. In this context, Table 6 shows that as



**Table 6**  
System capacity optimization results for each demand scenario.

Scenarios	PV rated capacity (kW)	<sup>a</sup> Converter capacity (kW)	Battery nominal capacity (kWh)	C <sub>C</sub> (\$/ml)	R <sub>C</sub> (\$/ml)	C <sub>O&amp;M</sub> (\$/ml)	TNPC (\$/ml)	LCOE (\$/kWh)
BC	375	450	600	1.010	1.244	0.185	2.439	1.205
S1	490	500	1000	1.776	2.184	0.246	4.206	0.887
S2	965	770	1350	2.240	3.166	0.459	5.865	0.592
S3	1260	1000	1745	3.070	3.755	0.578	7.403	0.404

<sup>a</sup> HOMER does not allow separate modeling of MPPT controllers, but they can be combined with the converter or the BESS. Therefore, the optimal MPPT size, in this analysis, is implicitly modeled with the converter.

**Table 7**  
Optimal capacity additions by component type for each scenario compared to the BC.

Scenarios	<sup>a</sup> PV	<sup>a</sup> Converter	<sup>a</sup> Battery bank
	Required additional capacity (kW)	Required additional capacity (kW)	Required additional capacity (kWh)
S1	115	50	400
S2	590	320	750
S3	885	550	1145

<sup>a</sup> The optimal capacity additions represent the newly added capacities to the existing system.

**Table 8**  
Comparison of life-cycle capacity addition costs (NPC) in each scenario by technology.

Scenarios	<sup>a</sup> PV	<sup>a</sup> Converter	<sup>a</sup> Battery	<sup>a</sup> Total system expansion	
	NPC (\$/ml)	NPC (\$/ml)	NPC (\$/ml)	TNPC (\$/ml)	% Change in TNPC to the BC
S1	0.330	0.143	1.294	1.767	72
S2	0.951	0.349	2.126	3.426	140
S3	1.715	0.677	2.572	4.964	203

<sup>a</sup> The capacity expansion costs represent the Net Present Cost of the added capacities over the lifetime of the MG.

the demand (and thus the generation capacity) expands from the BC scenario to S1, S2, and S3, the system’s TNPC increases by 72 %, 140 %, and 203 %, respectively, while the LCOE decreases by 26 %, 51 %, and 67 %, respectively.

Fig. 5a shows decreasing LCOE and increasing TNPC, as expected, with capacity additions. Fig. 5b depicts the PV/battery ratio (kWp/kWh), an important factor to consider when designing robust and reliable PV-battery systems (Warmuz & De Doncker, 2019; Weniger et al., 2014), in this CEP to range from 0.5 in S1 to 0.72 in S3. Particularly, in S2 and S3, the optimal PV/battery ratio of the system falls between 0.7

**Table 9**  
Electrical performance of the optimal generation capacity for each demand scenario.

Scenarios	Total electrical production (MWh/yr)	Total primary load served (MWh/yr)	Unmet electrical load (MWh/yr)	Unmet load fraction (%)	Total capacity shortage (MWh/yr)	Capacity shortage fraction	Total excess electricity (MWh/yr)	Peak load (kW)
BC	555	389	251	39.3	340	46.15	0	234
S1	880	580	60	9.39	114	10.0	0	361
S2	1352	1017	92	8.29	175	9.75	91	517
S3	1705	1400	88	5.92	221	7.66	116	620

**Table 10**  
Technical performances of the optimally expanded BESS in each scenario.

Scenarios	Nominal capacity (kWh)	Usable capacity (kWh)	Service life (yrs)	Battery autonomy (h)	Annual throughput (kWh/yr)	Storage depletion (kWh/yr)	Storage wear cost (\$/kWh)	Energy losses (kWh/yr)
BC	600	421	7.25	6.64	84,200	151	0.501	4344
S1	1000	700	8.71	12.1	153,000	188	0.342	4679
S2	1350	985	9.32	19.5	211,950	234	0.255	8348
S3	1745	1251	9.74	24.0	261,750	434	0.210	9870

and 1.88 kWp/kWh that earlier studies recommended for long-term capacity sizing of robust and reliable PV MG systems (Mandelli et al., 2016; Boeckl & Kienberger, 2019; Seel et al., 2020). Robustness in renewable MGs refers to the ability of the system to continue operating normally, without significant degradation in performance, despite disturbances, uncertainties, and changes in load demand, inputs, and energy resource conditions (Yang & Su, 2021).

The cash flow summary, shown for S2 in Fig. 6, displays that the C<sub>C</sub> and R<sub>C</sub> jointly make up most (92 %) of the TNPC. One explanation for this is that both the PV and the BESS have high initial C<sub>C</sub>. The other factor is that the BESS is consisted of several batteries, each of which has a short lifespan (10 years) and, hence, their R<sub>C</sub> constitutes sizable percentage of the TNPC. The low C<sub>O&M</sub> is largely due to the absence of fuel expenses and the low personnel salaries in Ethiopia.

*Optimal capacity additions and corresponding costs*

Table 7 presents the capacity additions required for the optimal system in each scenario compared to the BC. According to Table 7, compared to the BC, the PV array of the MG needs to be expanded by 30 %, 157 %, and 236 % in S1, S2, and S3, respectively; and the nominal battery capacity needs to increase by 67 %, 125 %, and 190 % in S1, S2, and S3, respectively. The converter capacity, in contrast, has to increase by 11 %, 71 %, and 122 % in S1, S2, and S3, respectively. The results reveal that the capacity expansion in all scenarios entails expanding both the PV and battery systems. The size of the capacity additions, nevertheless, differs markedly between scenarios and technologies. Unsurprisingly, the optimal system for S3 where the projected yearly energy demand is about four times the current supply level, requires the largest expansion of both the PV and batteries.

To determine the cost of capacity additions, the cash flows computed by HOMER for the optimal system and component sizes for each expansion pathway are utilized and compared. It should be noted that the expansion cost of each component includes the C<sub>C</sub>, R<sub>C</sub>, and C<sub>O&M</sub> of the component over the life-time of the MG. The results (Table 8), show that the battery capacity expansion entails a LCC ranging from \$1.294

**Table 11**  
Optimization results for a 100 % reliable system (all loads met at all times).

Scenarios	PV (kW)	Converter (kW)	Battery nominal (kWh)	Annual production (MWh/yr)	Total load served (MWh/yr)	TNPC (\$ml)	LCOE (\$/kWh)	Excess electricity (MWh/yr)	Peak load (kW)
S1	745	635	1250	1070	675	6.413	1.540	70	380
S2	1240	1110	1730	1598	1170	8.488	0.961	125	610
S3	1408	1298	2015	1946	1573	10.140	0.605	167	673

**Table 12**  
Electricity tariff rates in Ethiopia for the residential sector as of December 2021.

Tariff class (block)	Monthly electricity consumption (kWh)	Tariff per kWh (ETB)	Tariff per kWh (US\$)
1	Up to 50 kWh	0.2730	0.0052
2	Up to 100 kWh	0.7670	0.0145
3	Up to 200 kWh	1.6250	0.0307
4	Up to 300 kWh	2.0000	0.0377
5	Up to 400 kWh	2.2000	0.0415
6	Up to 500 kWh	2.4050	0.0454
7	Above 500 kWh	2.4810	0.0468

Source: EEU, 2022.

**Table 13**  
Financial profitability metrics of the capacity expansion in each scenario.

Metric	BC	S1	S2	S3
Return on investment (%)	-3.4	0.63	1.15	2.03
Discounted payback period (years)	>20	19.5	17.2	14.5

ml in S1 to \$2.572 ml in S3; and the PV array expansion involves a LCC ranging from \$0.33 ml in S1 to \$1.72 ml in S3. The findings unfold that in all scenarios, the battery and PV array expansion account for the majority of the total capacity expansion costs, with the battery expansion accounting for 52 % in S3, 62 % in S2, and 73 % in S1. By contrast, the PV array expansion cost accounts for 19 % to 35 % of the total capacity expansion costs.

*Technical performance of the optimized system capacities*

*Electrical performance*

The electrical performance results, Table 9, show that, compared with the 1065 kWh/day average electricity generation in the BC, the reinforced MG produces 2410 kWh/day, 3704 kWh/day, and 4670 kWh/day under the S1, S2, and S3 expansion pathways, respectively. Likewise, the total load served by the MG has risen by an additional 191 MWh/year, 628 MWh/year, and 1011 MWh/year in S1, S2, and S3 as

compared to the BC. The findings confirm that, compared to the BC, all the three expansion pathways result in a significant increase in daily and annual electricity production. Yet, the reinforced MG still has an annual unmet load fraction ( $f_{unmet}$ ) of 9.39 %, 8.29 %, and 5.92 %, in S1, S2, and S3, respectively. This demonstrates that in none of the capacity expansion pathways analyzed, the projected load is fully met, implying that in none of them there is a 100 % reliability, although in S3 most (94 %) of the specified load is met followed by S2 (91.7 %).

A major focus of this research is the dynamic load growth and how the different optimal systems behave over time and on yearly basis. Fig. 7 displays that the annual primary load served by the expanded MG evolves differently over time in the three expansion pathways. Noticeably, the annual load served by the MG in S2 and S3 during the first six years grows at a slow rate and the system’s reliability in relation to the demand is close to 100 % in both scenarios. Over the following six years (2029–2035), however, the annual load served by the MG grows sharply, especially in S3. At the same time, the system’s reliability falls to 92 %–98 % for S2 and 95 %–98 % for S3. After 2035, the growth in annual load served by the MG in S2 and S3 begins to significantly decline as the degradation of the PV and batteries accumulates and the demand keeps growing. As a result, the systems’ reliability drops sharply to 85–92 % for S2 and 89–95 % for S3.

In contrast, the annual primary load served in S1 remains relatively stable for the first 6 years with a reliability level of approx. 95 % before steadily declining over the next 12 years, with a reliability level ranging between 75 % and 95 %. The figure clearly shows that the load served and reliability of the optimal system under S2 and S3 during the first 6 years, subsequent 6 years, and last 8 years are significantly different. The sizable differences in annual load served and reliability of the MG between the three periods (see Fig. 7) suggest that a one-step expansion of the MG in S2 and S3 may result in oversizing of the system and underutilization of the MG capacity, particularly during the first 12 years. Therefore, a step-wise expansion, preferably a two-step expansion – one in 2023 and another in 2035 – might be more cost-effective. However, step-wise expansions are not without limitations. Given the MG’s remote location, the stepped expansion may incur additional costs for skilled personnel, transportation, equipment import taxes, and other transaction costs. On the other hand, the steady drop in load served in S1

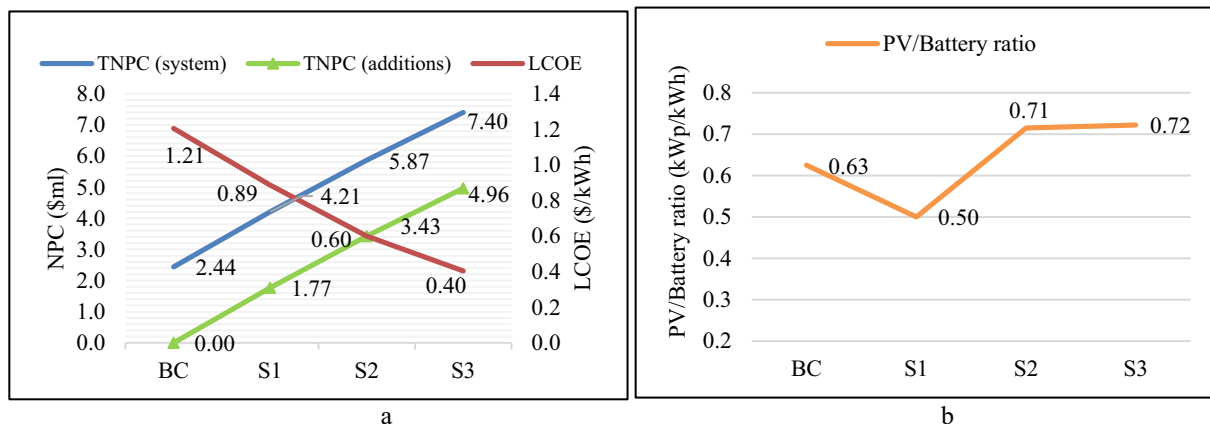


**Fig. 5.** Changes in the NPC and LCOE (a), and optimal PV/Battery ratio (b) of the MG as the capacity expands from BC to S-3, respectively.

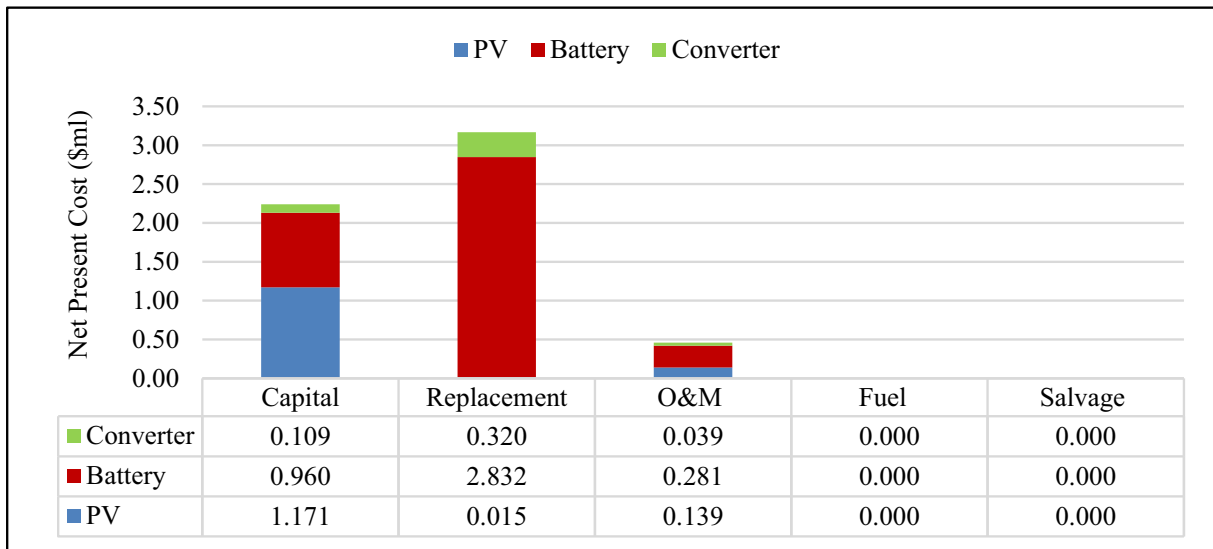


Fig. 6. Cash flow summary of the capacity expansion in Scenario 2, as an example.

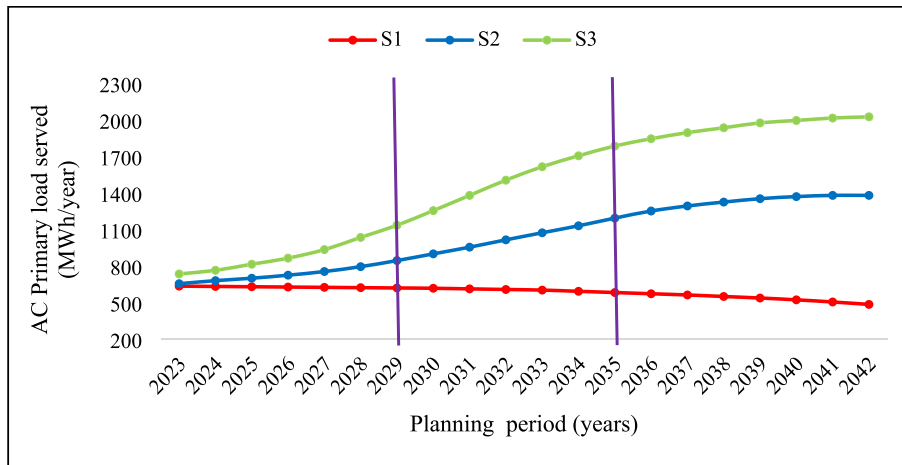


Fig. 7. Multi-year plot of the primary load served by the optimally expanded system in each case. The time span is divided into three phases.

suggests that a one-step expansion is most appropriate.

Fig. 8a and b, show the multi-year and hourly unmet load fractions ( $f_{unmet}$ ) of the optimal MG under each expansion pathway. Fig. 8a displays that in the first year (2023), the  $f_{unmet}$  is below 5 % in all three

expansion pathways. In the final year of the planning period (2042), however, the  $f_{unmet}$  in S1 and S2 expansion pathways has climbed to 24 % and 21.5 %, whereas it has reached to 16 % in S3. Fig. 8b shows that towards halfway the MG’s working life (2032), the expansion under S1

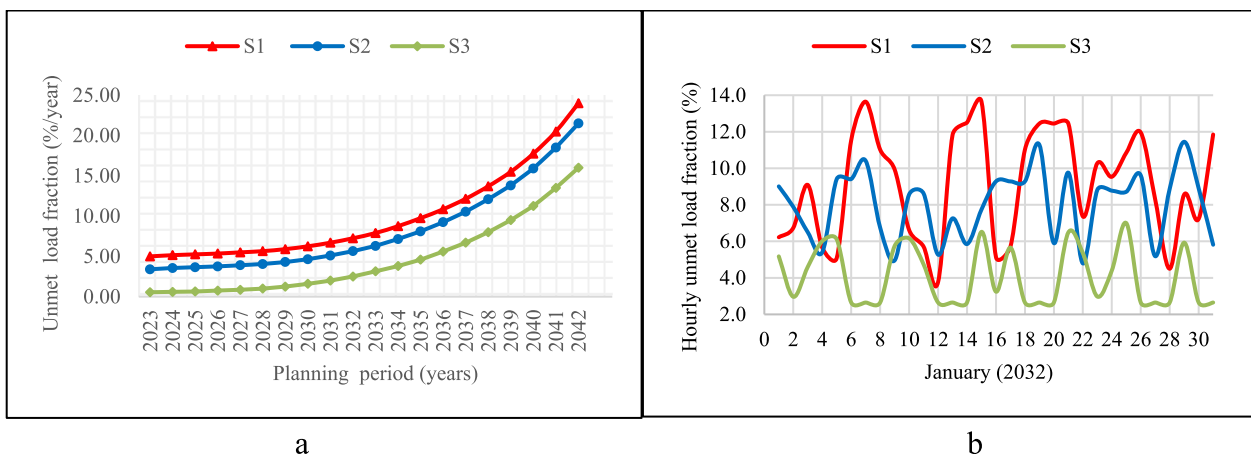


Fig. 8. Multi-year (a) and hourly (b) unmet load fraction (%) of the optimally expanded system under each scenario.

exhibits rather large hourly  $f_{\text{unmet}}$  (up to 14 %) that are characterized by sizable interday variability. In contrast, the hourly  $f_{\text{unmet}}$  of the expansion in S3, during the same year, is relatively low (mostly below 6 %) and stable. These results support the relative robustness and energy supply reliability of the optimal system configuration under the S3 expansion path.

#### Battery performance analysis

Off-grid renewable MGs rely on the BESS to serve nighttime loads and ease the unpredictability of power output with changes in solar irradiation and climatic conditions. The results of the BESS performance analysis using HOMER's advanced storage module (Table 10) show that, when the BESS's nominal capacity is increased from 600 kWh in the BC to 1745 kWh in S3, its service life, autonomy, and throughput improves by 2.5 years, 17.4 h, and 177, 550 kWh/year, respectively, while the storage wear cost decreases by \$0.29/kWh. Conversely, as the BESS size expands, the total annual energy losses and storage depletion increase due to the cumulative scale effect.

The technical performance analysis results, thus far, evince that the S3 capacity expansion where a 15 % annual increase in the electricity demand of productive users only is considered, lead to a relatively lower LCOE and higher supply reliability. Yet, even the S3 expansion pathway falls short of fully meeting the required load. In light of this, a separate optimization is performed with the reliability level set to 100 % (MACS = 0). The results, shown in Table 11, reveal that, compared to the optimal system achieved when the MACS is allowed to vary between 0 and 10 %, the TNPC of the 100 % reliable system rises by 52 %, 45 %, and 37 % in S1, S2, and S3, respectively. Following the same pattern, the LCOE surges by 74 %, 62 %, and 50 % in S1, S2, and S3, respectively. These findings prove that, raising the reliability of the MG, even under the S3 expansion path, from 94 % to 100 % elevates its TNPC and LCOE by 37 % and 50 %, respectively.

#### Economic performance analysis

Table 6 illustrates that the LCOE varies between the three expansion pathways, with S1 having comparatively the highest LCOE (\$0.887/kWh) and S3 the lowest (\$0.404/kWh). To further examine the temporal trend of the LCOE over the MG's lifetime, the LCOE is calculated for each year in each scenario by running iterative simulations in HOMER (i.e., by altering 'N' in Eq. (3)). The results, shown in Fig. 9, depict that during the first few years, the LCOE is highest in S3, but falls dramatically as the lifetime of the MG progresses and becomes the lowest beginning from 2029. Consistent with the load growth curves in Fig. 7, the LCOE in S2 and S3 is considerably different before and after 2029. In contrast, in S1 where the yearly demand growth rate is zero, the dynamics in LCOE over

time is marginal and slow. The graph demonstrates the relative long-term cost-effectiveness of the expansion under S3, where there is a rapid demand growth.

#### Financial profitability analysis

The EEU presently uses a highly-subsidized seven-slag tariff structure for HH users from all power sources, including MGs, based on the amount of electricity consumed per user per month as shown in Table 12. The data in Table 12 shows that the tariff rate ranges from \$0.0052/kWh for monthly consumption of up to 50 kWh to \$0.0468/kWh for monthly consumption of above 500 kWh. Based on the nearly two years of consumers data we obtained from the EEU, we calculated that the average electricity tariff for HH users in the study area is around \$0.030/kWh.

In light of the tariff rates in Table 12, we evaluated the financial profitability of the optimal system in each scenario by computing the return on investment (ROI) and the discounted payback period (DPP). HOMER calculates these investment appraisal metrics with reference to the BC. The results, presented in Table 13, indicate that compared to the BC, the S3 expansion exhibits a ROI of 2 % and a DPP of 14.5 years, suggesting that the MG may recover the entire investment costs (and hence the capacity expansion costs) within 15 years. In contrast, the MG in S1 and S2 shows a ROI of <2 % and a DPP longer than 17 years, suggesting that the MG under these two expansion pathways must operate for >17 years to reach break-even. Combining the tariff rates in Table 12 with the investment appraisal findings in Table 13 reveals that the MG is currently operating at a net loss and cannot recover the investment cost within the planning period, whereas the capacity expansions under S2 and S3 could turn a profit. However, it should be noted that HOMER only considers the energy production system when calculating the financial profitability of MG systems, ignoring the distribution and end-use system costs. As a result, even while the expansion in S2 and S3 indicate positive return on investment, this may not be the case in practice. This is because the additional costs for the development, management, and maintenance of power distribution systems to reach the new customers could significantly increase the total cost of the system and negatively affect its financial viability. The financial unviability is even more apparent when we compare the average electricity price above (\$0.030/kWh) with the calculated LCOE for the S3 (\$0.404/kWh). The comparison clearly reveals that, given the current tariff rate, the revenues collected from power sales may never recover the cost of MG expansion, even for the expansion under S3.

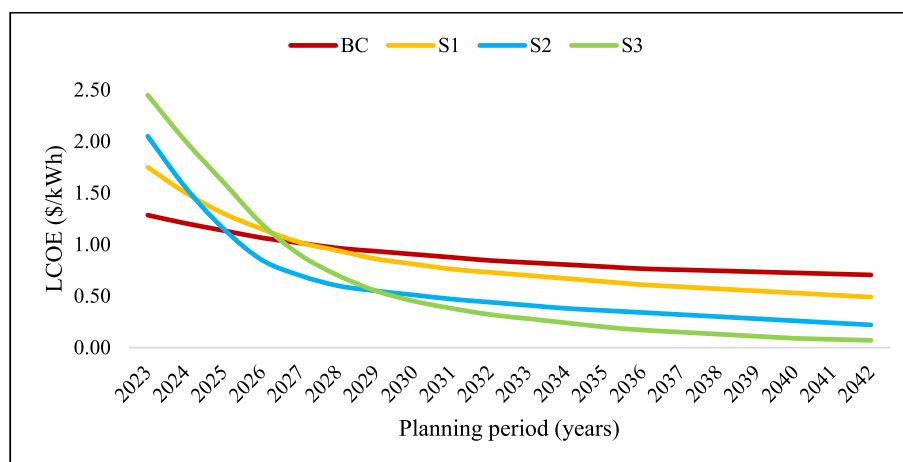


Fig. 9. Dynamics of the LCOE for each scenario over the 20-year planning horizon.

## Sensitivity analysis

### The maximum annual capacity shortage

To understand the technical and economic behavior of the expanded MG with changes in MACS, the S3 system is analyzed, as an example. The results, shown in Fig. 10a and b, reveal that, keeping all other model constraints constant, the TNPC and LCOE decline with increasing MACS, while the  $f_{\text{unmet}}$  rises. According to Fig. 10, reducing the MACS in S3, from 10 % to 0 %, hikes the TNPC and LCOE up by 108 % and 145 %, respectively. However, reducing the MACS of the same system from 10 % to 5 % only increases the TNPC and LCOE by 53 % and 64 % respectively. The explanation is that a 5 % reduction in the MACS gives the MG expansion planner more options to choose the right size, inexpensive batteries to supply all but the peak load, rather than using large-sized batteries to meet the entire load at all times. The results uphold that capacity expansion costs, LCOE and load served by the MG are all highly impacted by the level of the MACS.

### Ambient temperature and battery depth of discharge

The Omorate town experiences high temperatures during most days of the year. One of the serious issues identified by a recent study (Wassie & Ahlgren, 2023a) on the same MG was that the battery frequently discharges power at high DOD. Thus, it is vital to analyze the behavior of the expanded MG with changes in  $T_a$  and DOD. Fig. 11a shows that when the  $T_a$  increases from 24 °C to 48 °C, the PV production in S2, for example, drops by 690MWh/year (53 %) while the LCOE increases by 128 %. Fig. 11b illustrates that, in all scenarios, the battery's cycle life is significantly impacted by the DOD. However, the cycle life shortens more drastically in S1 than in S2 and S3, as the DOD increases.

The significantly reduced cycle life of the battery in S1 even when operating at the same DOD as the batteries in S2 and S3 shows that factors other than the DOD also affect battery cycle life. One such factor is temperature. Though an increase in temperature increases battery available capacity, higher battery operating temperatures (typically +55 °C) drastically shorten battery service life (Bhattacharyya et al., 2014). And this effect is more pronounced in small capacity BESS compared to large capacity BESS since large capacity battery packs can better withstand the effects of the high operating temperatures on the battery's chemical activity (Ouyang et al., 2020). A related factor is the battery charging rate. Frequent and fast battery charging accelerates battery degradation and reduces battery cycle life (Xie et al., 2020), and the larger the battery capacity relative to the load the less the battery operates at very low and very high SOC. This results in that less frequent and steady battery charging rates prolong the battery cycle life (Bhattacharyya et al., 2014). It is therefore possible that, despite having the same DOD as in S2 and S3, the battery in S1 is degrading more quickly from the high temperatures in Omorate as well as from charging and recharging multiple times a day at higher rates than the batteries in S2

and S3. This results in shorter cycle life of the battery in S1 than the batteries in S2 and S3. The findings demonstrate that under high DOD in a hot equatorial climate, even a cost-optimal battery capacity addition may not be sufficient to overcome the battery degradation problem.

### Real interest rates

The real interest rate (RIR), also called the real discount rate (RDR) is another important variable that affects the cost-effectiveness of capacity expansion investments in power systems. According to our analysis results, both the TNPC and the LCOE of the capacity expansion are sensitive to the RIR and the level of sensitivity varies across the three scenarios. A doubling of the RIR from 7 % to 14 % skyrockets the LCOE by 138 % in S2 and by 227 % in S3. The significant impact of the RIR on the LCOE in renewable power systems stems from the fact that a sizable portion of the electricity generation cost is due to the initial investment  $C_c$ . As such, the higher the RDR, the lower the present value of future cash flows (revenues), resulting in higher present costs per kWh.

## Discussion

Several important findings emerge from this study. First, under different capacity expansion paths, PV MG system configurations differ significantly in terms of component sizes, required capacity additions, technology costs and LCOE. It is found that for lower annual demand growth rates, the expansion results in higher LCOE, while for higher demand growth rates the expansion leads to a significantly lower LCOE. Evidently, expanding the current MG capacity to satisfy a 300 % higher demand compared to the BC, under the constraints and uncertainties considered, could reduce the LCOE by \$0.8/kWh (67 %). However, achieving this level of generation capacity and reducing the LCOE incurs significant investment, potentially elevating the MG's TNPC to >200 %. Fig. 5a illustrates that the TNPC of the system and the capacity additions both increase linearly with increase in the MG capacity. This is due - in large part - to the high  $R_c$  of batteries, given their relative short lifespan, compared to the PV array.

Second, the robustness and reliability of the optimal system configurations in the face of changes in load and uncertainties in other input variables are distinct under the three expansion pathways. The S3 expansion path, in particular, has demonstrated a low  $f_{\text{unmet}}$ , and LCOE, despite the sizable yearly demand growth, uncertainty in input variables and PV degradation rates taken into account. This indicates the relative reliability of the S3 system in terms of satisfying most of the projected demand without load shedding, as well as the system's robustness against changes in temperature, PV and battery degradations, and load fluctuations. This is more apparent in Fig. 8b where the increased robustness in S3 has imparted resilience to the MG's operation resulting in significant reduction of the jumps in the  $f_{\text{unmet}}$  curve compared to the  $f_{\text{unmet}}$  curves in S1 and S2. The results establish the importance of taking

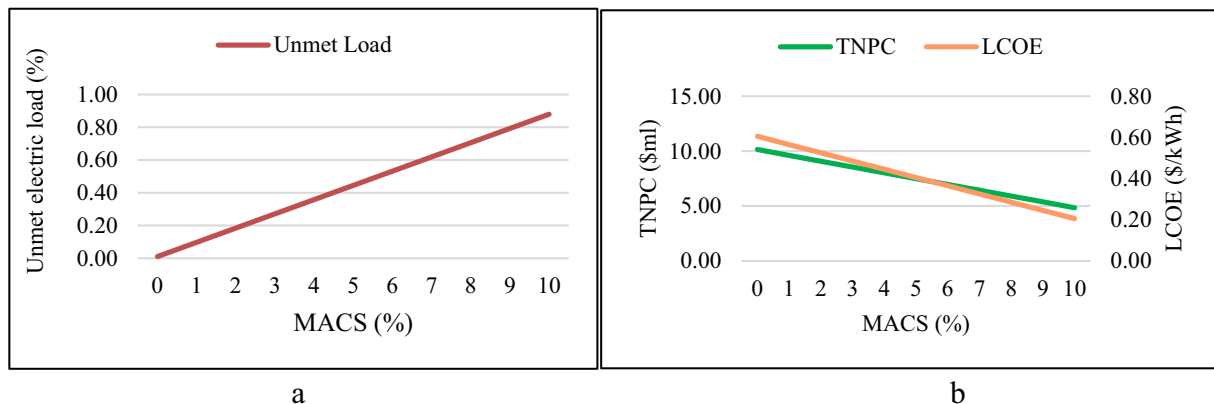


Fig. 10. Sensitivity of the unmet load fraction (a) and TNPC and LCOE (b) of the reinforced MG under the S3 expansion to changes in MACS.

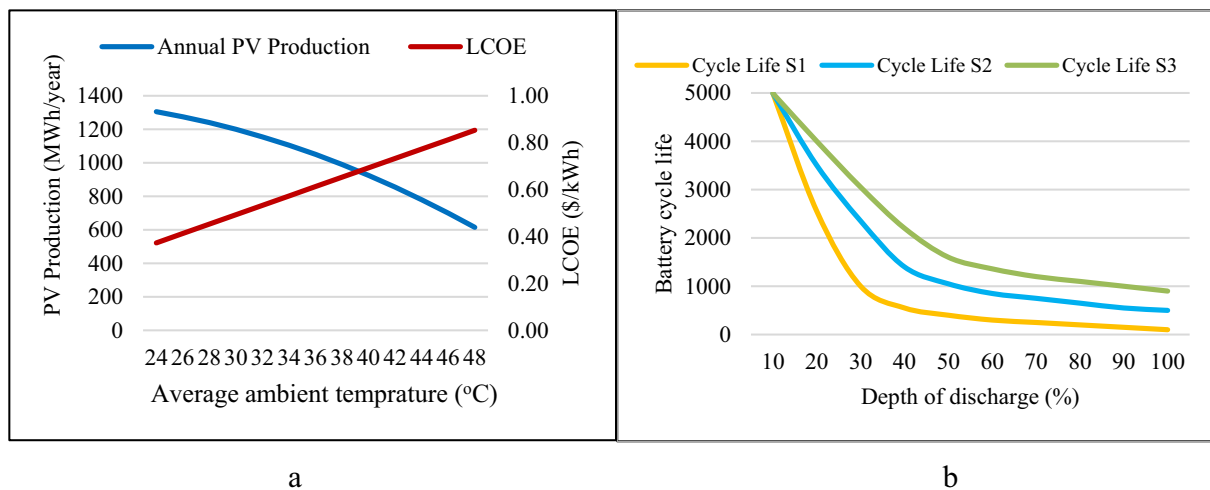


Fig. 11. Sensitivity of PV production and LCOE (a), and Battery cycle life (b) of the optimally expanded system to changes in the ambient temperature and battery DOD, respectively.

into account various demand growth scenarios and uncertainties in CEP to determine the most robust and reliable MG configuration.

A useful indicator for robustness of CEP in PV-battery MGs is the PV/battery ratio ( $\text{kW}_{\text{peak}}/\text{kWh}$ ). In this regard, the results show that the PV/battery ratio is 0.71  $\text{kWp}/\text{kWh}$  in S2 and 0.72  $\text{kWp}/\text{kWh}$  in S3. A previous study (Boeckl & Kienberger, 2019) for households in Austria determined that for a self-sufficiency level of 70 % or higher, the optimal PV/battery ratio for a grid-tied home-scale PV system ranges from 0.76 to 1.88  $\text{kWp}/\text{kWh}$ . Using data from 46 operating large-scale PV power plants in the US, Steel (Seel et al., 2020) calculated the average PV/battery ratio to be 1.28. In rural SSA, Mandelli et al. (Mandelli et al., 2016) suggested that a PV/battery ratio of approx. 0.7 ( $\text{kWp}/\text{kWh}$ ) should be considered for reliable small-scale PV installations. In light of these prior studies, the PV/battery ratios found in this study are lower when compared to those found in Austria (Boeckl & Kienberger, 2019) and the US (Seel et al., 2020), but are in line with the recommendations for rural SSA. Given the lack of rigorous studies on optimal CEP of MGs in SSA, the PV/battery ratios found in this study could, thus, serve as a benchmark for designing robust PV MGs.

Another interesting finding is that, in S1 the largest expansion is performed on the battery. This indicates that the inability of the existing system to fully meet the current load requirement is due more to the limited capacity and poor performance of the BESS than the PV's generation capacity shortfall. As noted earlier, the MG is situated in a hot semi-arid equatorial climate with the annual maximum temperature ranging from 35.2 °C to 42.8 °C (Wassie & Ahlgren, 2023b). This significantly impacts both the PV cells efficiency and the batteries cycle life. As a result, the optimal system for S1 shows a relatively large increase in the battery capacity. The takeaway is that in hot tropical regions with extended nighttime peak loads, deliberate oversizing of the BESS capacity might be necessary to reduce the number of hours the battery operates in the high SOC range and, as a result, enhance its energy output and cycle life. The findings support a prior study in tropical India (Bonkile & Ramadesigan, 2022) which showed that battery sizing has significant impact on the battery's service life and power generation in PV MGs.

The electrical performance analysis reveals that expanding the MG capacity to fully meet the load at all times ( $f_{\text{unmet}} = 0$ ) is possible, but it would be prohibitively costly. As noted by Bhattacharyya et al. (Bhattacharyya et al., 2014), it is always recommended to use larger capacity batteries to meet a given electrical load. However, a larger battery also increases system costs. Conversely, expanding the MG solely based on cost minimization may not produce the desired reliability. This highlights the significant non-linear trade-off between minimizing capacity

expansion costs and maximizing reliability levels of off-grid PV MGs. Therefore, sacrificing some level of reliability (MACS = 0 to 5 %) is unavoidable and necessary to minimize the trade-off and temper the expansion costs. Capacity expansion of isolated MGs with MACS = 0 can also result in considerable excess power production, (Table 11), which leads to diminished capital recovery as the excess power cannot be exported to the national grid. In line with our findings, a study on an off-grid PV MG in Malawi (Louie & Dauenhauer, 2016) found that increasing the system's reliability from 99 % to 100 % increased its TNPC by 46 %.

The consistently decreasing LCOE trajectory in S3 in Fig. 9 illustrates that, in the long-run, the revenues generated from the increased power production could offset the capacity expansion costs. Further, the graph purports that, given there is adequate demand for the power produced, capacity expansion becomes more cost-effective as the demand evolves i.e., economy of scale. According to the results, the expansion strategy that supports productive use of electricity (S3) improves the cost-effectiveness of the capacity expansion. This result has important policy implications in that it unveils that the development off-grid PV MGs to meet the demand from productive use increases their bankability. Notwithstanding, under the current electricity tariff rates in Ethiopia, none of the expansion pathways analyzed appear to be financially viable. As shown in the financial analysis, the average electricity price for HH users in the study area is about \$0.030/kWh. Comparing this price to the LCOE calculated for the S3 (\$0.404/kWh) reveals that the revenues generated from power sales may not be able to recover the cost of MG expansion. To further verify this, we made a simple calculation of the total capacity expansion costs per unit of increase in the MG's electricity output for S3. We discover that for every 1 kWh of PV production increase compared to the BC, a lifetime system capacity expansion cost of \$0.15 is involved.

The findings highlight two important points. First, the financial viability of MG capacity expansion heavily depends on the electricity prices. Second, ensuring the financial viability of off-grid MGs in Ethiopia requires designing the systems to support productive use of electricity and introducing appropriate incentive mechanisms and tariff restructuring. This is particularly relevant for private renewable MG developers in order to counter the disincentive from the current low tariff rates. Contrary to our findings, a CEP for a grid-tied MG in New Zealand (Mohseni et al., 2020) showed that the existing tariff rate (NZ \$0.08/kWh) could effectively recover the costs of the planned capacity expansion.

The sensitivity analysis results show that the  $f_{\text{unmet}}$ , NPC and LCOE of the optimally expanded MG significantly change with changes in the

MACS. The ambient temperature ( $T_a$ ) and battery's DOD are other major factors found to significantly affect the PV output and battery cycle-life, and hence the LCOE and performance of the capacity expansion. This is evident in Fig. 11a, where a 100 % increase in the  $T_a$  reduces the annual PV production by 53 %. The results strengthen earlier studies (Jufri et al., 2021; Dash & Gupta, 2015; Limmanee et al., 2017) which found that higher  $T_a$  in tropical climates significantly reduces PV power output and battery life by accelerating degradation and dropping PV cells efficiency. These findings have of paramount importance since they reveal the profound effects of controllable and uncontrollable factors on the cost and operational performance of PV MGs in tropical areas, and that these effects must be considered by expansion planners at the outset of the system design and CEP. Overall, this work provides some crucial insights into the complexity of capacity expansion of off-grid PV MGs. Although not all, many of the findings of the study have a high degree of generalizability to the context in tropical east Africa and other developing regions at large. These applicable findings include the significant non-linear trade-offs between capacity expansion costs and reliability, the large differences in capacity expansion costs and LCOE among different load growth patterns, the significant effects of changes in input variables and exogenous factors such as temperature on the techno-economic performance of the optimally expanded MG systems, and the significance of satisfactory electricity tariff rates in the cost recovery of MG capacity expansion.

#### Limitations of the study

Although a multi-year optimization approach with yearly varying demand is used to determine the optimal MG capacity in each scenario, the capacity expansion is attained through a single-phase capacity addition approach rather than a multi-phase or step-by-step expansion strategy, in which the MG capacity is expanded in several phases over time. The main reason that we were unable to use a multi-step expansion approach is that HOMER does not have any built-in tools to do that yet. According to some studies (Sayani et al., 2022), a multi-step capacity expansion can reduce the total expansion cost by up to 12 % when compared to a single-step capacity expansion approach. Another limitation of this study is that HOMER only considers the energy production system when determining the financial profitability of MGs, essentially disregarding the distribution and end-use system costs. As a result, even when capacity expansions show positive investment return, this may not be the case in reality due to considerable unaccounted additional power distribution and end-use system costs associated with new customers.

#### Conclusions

A long-term optimal capacity expansion planning (CEP) was carried out for a burdened off-grid PV-battery mini-grid (MG) installed in a remote small town in Ethiopia. The aim of the CEP was to determine the long-term optimal capacity additions to meet the required load and reliability at the lowest cost possible, under different energy demand growth scenarios: 0 % (meets the minimum required load), 5 %, and a 15 % for productive users only. The CEP was performed using HOMER Pro's multi-year optimization tool over a 20-year planning period. In all scenarios, the generation mix consisted of only solar energy and the maximum allowable annual capacity shortage (MACS) was restricted to 10 %. The actual total load served by the MG in 2022 was used as a reference or base case (BC) scenario. The performance of the optimally reinforced MG system in each of the three scenarios was then compared to the BC using technical, economic, and financial metrics.

Our findings show that the expansion path, which allows for a 15 % annual power demand growth from productive users only, requires the largest capacity expansion. Component-wise, the battery and PV systems require the largest expansions in all scenarios. In all the expansion paths analyzed, the battery capacity expansion cost accounted for most (52 to 73 %) of the total capacity expansion costs followed by the PV array (19

to 35 %). The average cost per kWh of electricity (LCOE) of the optimally expanded MG ranged from \$0.404/kWh in scenario-3 to \$0.887/kWh in scenario-1. It was found that, the expansion in scenario-3 is relatively cost-effective and fulfils most (94 %) of the projected load demand even in the presence of constraints. However, it comes at a substantial cost and still leaves 6 % of the load unmet. The energy, economic and sensitivity analyses clearly showed that a thorough accounting of demand evolution and uncertainties in input variables over time is critical to achieving a robust MG capacity expansion that reliably meets the load.

There are many important conclusions to be drawn from this study. First, the study demonstrated that capacity expansion of PV MGs is characterized by significant trade-offs between expansion costs and reliability. On the one hand, MG capacity expansion based solely on cost-minimization may not ensure maximum reliability. On the flipside, capacity expansion with 100 % reliability incurs overly high cost, highlighting that it is practically impossible to achieve 100 % reliability without suffering a substantial loss in cost-effectiveness of the capacity expansion. As such, some degree of reliability must be forfeited to realize a doable capacity expansion at a reasonable cost, subject to budgetary, operational, and other constraints. Second, the load served by the optimally expanded MG evolves differently over time and on an annual basis between the different expansion pathways and, therefore, the expansion strategy (one-step or multi-step) must take into account the dynamic load growth pattern. A related finding is that the reliability and LCOE of MG capacity expansion varies markedly depending on the annual load growth rate, with the maximum reliability and lowest LCOE being attained from the expansion pathway that handles the highest annual load growth rate and productive use of electricity. Third, the performance and cost-effectiveness of MG capacity expansion is strongly affected by uncertainties in input variables and the extent to which these uncertainties are accounted for during the planning process. Higher ambient temperatures and battery DOD, in particular, stand out as having a significant negative effect on the performance and cost of the capacity expansion by affecting the PV power output and battery life. Fourth, low electricity tariff rates render solar PV based rural electrification initiatives in the developing world financially unviable and discourage the private sector from taking part. This work makes two major contributions. First, it advances knowledge and understanding on long-term CEP of off-grid PV MGs under dynamic demand in the context of tropical regions. Second, it assists policy makers, MG designers and private entrepreneurs in assessing the complex non-linear trade-offs between capacity expansion costs and reliability levels of off-grid PV MGs.

#### CRedit authorship contribution statement

**Yibeltal T. Wassie:** Conceptualization, Methodology, Field data collection and investigation, Formal analysis, Writing - original draft, and Writing - review and editing.

**Erik O. Ahlgren:** Conceptualization, Methodology, Resources, Writing - review and editing, Visualization, Supervision, Project administration, and Funding acquisition.

#### Declaration of competing interest

The authors declare that they have no known competing financial interests or personal relationships that could have appeared to influence the work reported in this paper.

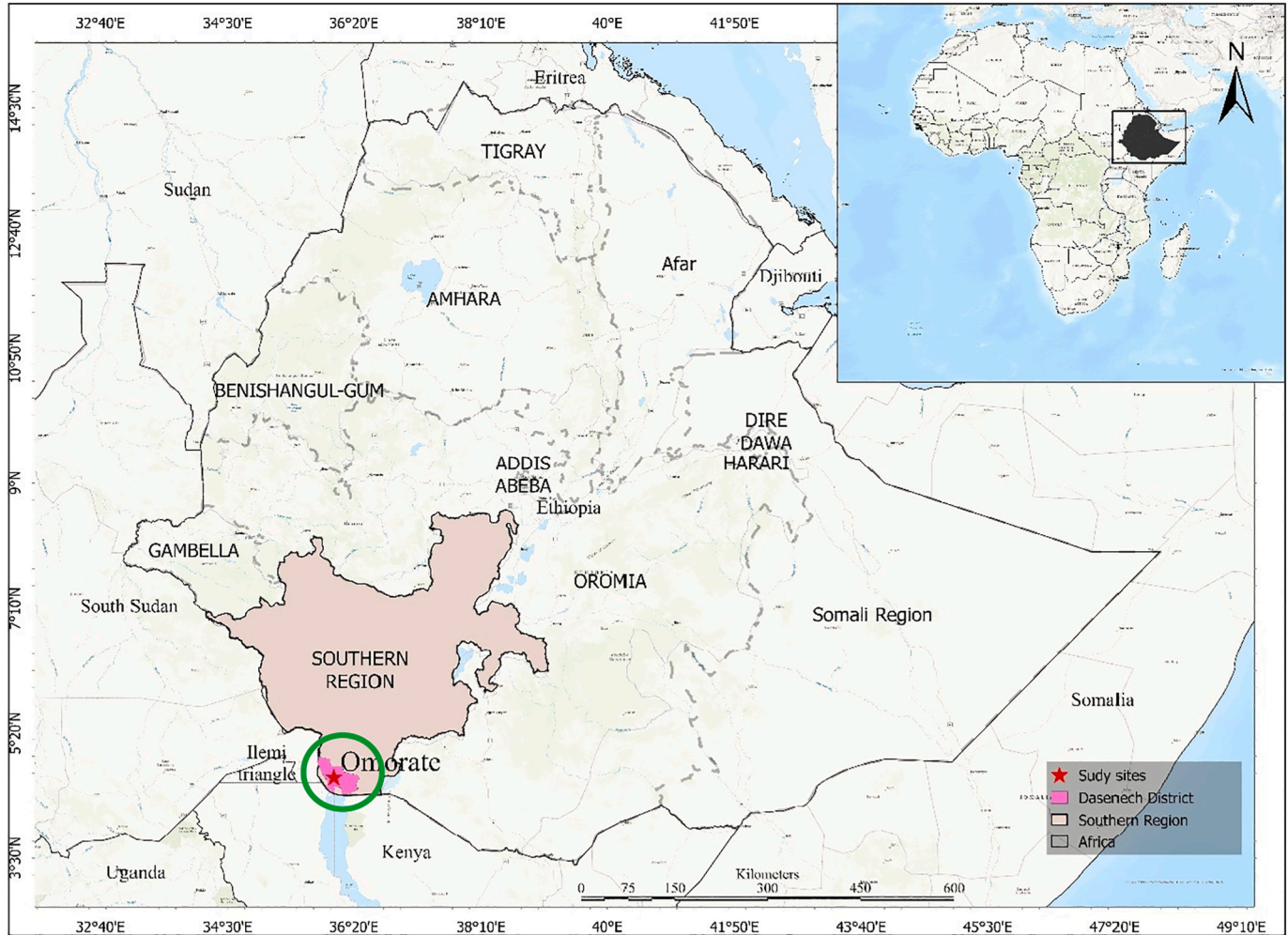
#### Acknowledgment

The authors wish to acknowledge the Swedish Research Council and the Chalmers University of Technology Energy Area of Advance for providing financial assistance to conduct this research. The authors would also like to express their gratitude to the Ethiopian Electric Utility

(EEU), the coordinators of the Universal Electricity Access Program (UEAP) at Hawassa and Arba-Minch and the mini-grid operators at

Omorate for their support and facilitation of the data collection.

**Appendix A. Location map of the PV mini-grid at Omorate, southern Ethiopia**



**Appendix B. The PV mini-grid infrastructure at Omorate, southern Ethiopia**





**Appendix C. Technical specification of the existing hybrid mini-grid system**

Component	Parameters	Specification
Geographic location	Omorate, Dasanech district, Southern Ethiopia	
	Latitude	4° 8' 16"N
	Longitude	36° 3'29" E
	Elevation	368 m. a.s.l.
	Mean annual ambient temperature	29.2 °C
Installation	Fixed ground-mounted racks	
	AC-coupled with 9 strings in two parallel rows	
Configuration PV array	PV module type Mono-PERC (mono-crystalline)	JKM310M-60-MX
	Number of PV cells per module	60
	Total number of PV modules	1210
	PV module dimension (Length x Width)	1.65 cm × 0.992 cm
	Total effective area of the PV array	1980.5 m <sup>2</sup>
	Tilt angel	15° facing south
	Maximum power per unit of area at STC	189.4 W/m <sup>2</sup>
	Rated output power per module	310 Wp
	Global Horizontal Irradiation	5.904 kWh/m <sup>2</sup> /day
	Measured irradiation at the tilted plane	6.07 kWh/m <sup>2</sup> /day
	Module conversion efficiency at STC	18.94 %
	Total installed/rated PV capacity	375 kWp
	PV lifetime	25 years
	Temperature coefficient	-0.40 %/°C
	Converter	Converter model
Total Number of inverters		9
Max input power (DC) of each inverter		75kWp
Max output power (AC) of each inverter		50 kWp
Nominal voltage		585 V
Max. AC apparent power (kVA)		55.5kVA
Converter output AC voltage		220/380 VAC three-phase
Max output current		80.5A
Lifetime		10 years
Maximum efficiency		96 %
Energy storage (battery)	Nominal Voltage	384 V
	Nominal capacity	1500 Ah
	Battery type	Pack

(continued on next page)

(continued)

Component	Parameters	Specification
Diesel generator (DG)	Max energy storage capacity	600 kWh
	Number of battery blocks/racks	5 × 60 kW
	Battery cell chemistry	LiFePO <sub>4</sub>
	Minimum charge/discharge life cycles	5000 cycles
	Max lifetime per battery	10 years
	Round trip efficiency (%)	80
	Battery cell energy density	125 Wh/kg
	DC power supply voltage	24 V
	Rated output power (kVA/kW)	125/100
	DG output AC voltage	220/380 VAC three-phase
	Load minimum ratio	30 %
	Minimum fuel efficiency	32 %

**Appendix D. A daily load report of the existing MG for a typical weekday in December 2022**

Site:	OMORATE						Date: 2022-12-29					
Time	Load 1						Load 2					
	Ia(A)	Ib(A)	Ic(A)	P(kW)	Q(kVar)	COS	Ia(A)	Ib(A)	Ic(A)	P(kW)	Q(kVar)	COS
00:00	0	0	0	0	0	0.00	0	0	0	0	0	0.00
01:00	0	0	0	0	0	0.00	0	0	0	0	0	0.00
02:00	0	0	0	0	0	0.00	0	0	0	0	0	0.00
03:00	0	0	0	0	0	0.00	0	0	0	0	0	0.00
04:00	0	0	0	0	0	0.00	0	0	0	0	0	0.00
05:00	0	0	0	0	0	0.00	0	0	0	0	0	0.00
06:00	0	0	0	0	0	0.00	0	0	0	0	0	0.00
07:00	0	0	0	0	0	0.00	0	0	0	0	0	0.00
08:00	0	0	0	0	0	0.00	0	0	0	0	0	0.00
09:00	159	145	157	93	52	0.87	0	0	0	0	0	0.00
10:00	161	161	172	99	55	0.88	0	0	0	0	0	0.00
11:00	169	165	167	102	55	0.88	0	0	0	0	0	0.00
12:00	155	165	159	98	52	0.89	0	0	0	0	0	0.00
13:00	172	166	175	105	53	0.89	0	0	0	0	0	0.00
14:00	163	158	166	98	52	0.89	0	0	0	0	0	0.00
15:00	167	164	182	105	55	0.88	0	0	0	0	0	0.00
16:00	152	156	158	93	53	0.88	0	0	0	0	0	0.00
17:00	156	150	158	93	53	0.87	0	0	0	0	0	0.00
18:00	0	0	0	0	0	0.00	0	0	0	0	0	0.00
19:00	0	0	0	0	0	0.00	0	0	0	0	0	0.00
20:00	191	179	196	121	46	0.93	0	0	0	0	0	0.00
21:00	176	172	164	108	45	0.92	0	0	0	0	0	0.00
22:00	0	0	0	0	0	0.00	0	0	0	0	0	0.00
23:00	0	0	0	0	0	0.00	0	0	0	0	0	0.00
24:00	0	0	0	0	0	0.00	0	0	0	0	0	0.00

**Appendix E. Energy demand growth scenarios (MWh/year) considered for the capacity expansion planning over the 20-year planning period**

Year	Base case scenario	Scenario 1	Scenario 2	Scenario 3
2023	389	639	671	687
2024	389	639	704	738
2025	389	639	740	794
2026	389	639	777	853
2027	389	639	816	917
2028	389	639	856	986
2029	389	639	899	1060
2030	389	639	944	1140
2031	389	639	991	1225
2032	389	639	1041	1317

(continued on next page)

(continued)

Year	Base case scenario	Scenario 1	Scenario 2	Scenario 3
2033	389	639	1093	1416
2034	389	639	1148	1522
2035	389	639	1205	1636
2036	389	639	1265	1759
2037	389	639	1328	1891
2038	389	639	1395	2033
2039	389	639	1465	2185
2040	389	639	1538	2349
2041	389	639	1615	2525
2042	389	639	1695	2714
<b>Annual average</b>	<b>389</b>	<b>639</b>	<b>1109</b>	<b>1487</b>
<b>Daily average</b>	<b>1065</b>	<b>1750</b>	<b>3039</b>	<b>4075</b>

## References

- Allee, A., et al. (2021). Predicting initial electricity demand in off-grid Tanzanian communities using customer survey data and machine learning models. *Energy for Sustainable Development*, 62(4), 56–66.
- Amara, S., et al. (2021). Improvement of techno-economic optimal sizing of a hybrid off-grid micro-grid system. *Energy*, 233(C).
- Asress, M. B., et al. (2013). Wind energy resource development in Ethiopia as an alternative energy future beyond the dominant hydropower. *Renewable and Sustainable Energy Reviews*, 23, 366–378.
- Bhattacharyya, S. C., Palit, D., & Kishore, V. V. N. (2014). Suite of off-grid options in South Asia. In S. C. Bhattacharyya, & D. Palit (Eds.), *Mini-grids for rural electrification of developing countries: Analysis and case studies from South Asia* (pp. 82–88). Springer International Publishing.
- Boeckl, B., & Kienberger, T. (2019). Sizing of PV storage systems for different household types. *Journal of Energy Storage*, 24, Article 100763.
- Bonkile, M. P., & Ramadesigan, V. (2022). Effects of sizing on battery life and generation cost in PV–wind battery hybrid systems. *Journal of Cleaner Production*, 340, Article 130341.
- Boruah, D. (2020). *Developing solar PV mini-grid projects - key design considerations*. New Delhi: Global Sustainable Energy Solutions India. <https://www.linkedin.com/pulse/developing-solar-pv-mini-grid-projects-key-design-dwipen-boruah> (accessed on 15.03.2023).
- Brooks, A. E. (2014). Solar energy. In *Future energy* (2nd ed., pp. 383–404).
- Dash, P. K., & Gupta, N. C. (2015). Effect of temperature on power output from different commercially available photovoltaic modules. *International Journal of Engineering Research and Applications*, 5, 148–151.
- Dawood, F., Shafiqullah, G. M., & Anda, M. (2020). Stand-alone microgrid with 100% renewable energy: A scenario study with hybrid solar Pv-battery-hydrogen. *Sustainability*, 12, 2047.
- EEU (2022). Ethiopian Electric Utility: Projects Portfolio Management Directorate. <http://www.ethiopianelectricutility.gov.et/news/detail/191?lang=en> (Accessed 24 January 2022).
- ESMAP. (2022). Energy sector management assistance program. In *Mini-grids for half a billion people: market outlook and handbook for decision makers*. Washington, DC: World Bank.
- Fioriti, D., et al. (2018). Stochastic sizing of isolated rural mini-grids including effects of fuel procurement and operational strategies. *Electric Power Systems Research*, 160, 419–428.
- Gabra, S., Miles, J., & Scott, S. A. (2019). Techno-economic analysis of stand-alone wind micro-grids, compared with PV and diesel in Africa. *Renewable Energy*, 143, 1928–1938.
- Groissböck, M., & Gusmão, A. D. (2017). Reliability constrained least-cost generation expansion planning: An isolated mini-grid in KSA. *ArXiv, Physics and Society*, 1, 1–14.
- Han, H., et al. (2018). Degradation analysis of crystalline silicon photovoltaic modules exposed over 30 years in hot-humid climate in China. *Solar Energy*, 170, 510–519.
- Hartvigsson, E., Stadler, M., & Cardoso, G. (2018). Rural electrification and capacity expansion with an integrated modeling approach. *Renewable Energy*, 115, 509–520.
- Hartvigsson, E., et al. (2021). Linking household and productive use of electricity with mini-grid dimensioning and operation. *Energy for Sustainable Development*, 60, 82–89.
- HOMER Energy. (2022). *HOMER pro version 3.15.3. User manual*. Boulder, CO, USA: HOMER Energy (released August 10, 2022).
- IEA, et al. (2022). *Tracking SDG 7: The Energy Progress Report*. Washington, D.C.: The World Bank.
- Jufri, F. H., et al. (2021). Optimal battery energy storage dispatch strategy for small-scale isolated hybrid renewable energy system with different load profile patterns. *Energy*, 14, 3139.
- Khatib, T., Sopian, K., & Kazem, H. A. (2013). Actual performance and characteristic of a grid connected photovoltaic power system in the tropics: A short term evaluation. *Energy Conversion and Management*, 71, 115–119.
- Lambert, T. (2006). Micropower system modeling with HOMER. In F. A. Farret (Ed.), *2006. A chapter in book: Integration of alternative sources of energy*. John Wiley & Sons, Inc.
- Limmanee, A., et al. (2017). Degradation analysis of photovoltaic modules under tropical climatic conditions and its impacts on LCOE. *Renewable Energy*, 102, 199–204.
- Lorenzoni, L., et al. (2020). Classification and modeling of load profiles of isolated mini-grids in developing countries: A data-driven approach. *Energy for Sustainable Development*, 59, 208–225.
- Louie, H., & Dauenhauer, P. (2016). Effects of load estimation error on small-scale off-grid photovoltaic system design, cost, and reliability. *Energy for Sustainable Development*, 34, 30–43.
- Mandelli, S., et al. (2016). The role of electrical energy storage in sub-Saharan Africa. *Journal of Energy Storage*, 8, 287–299.
- McCarthy, R. W., Ogdan, J. M., & Sperling, D. (2007). Assessing reliability in energy supply systems. *Energy Policy*, 35(4), 2151–2162.
- Mohseni, S., Brent, A. C., & Burmester, D. (2020). Community resilience-oriented optimal micro-grid capacity expansion planning: The scenario of totarabank eco-village, New Zealand. *Energies*, 13(15).
- Moner-Girona, M., et al. (2018). Electrification of Sub-Saharan Africa through PV/hybrid mini-grids: Reducing the gap between current business models and on-site experience. *Renewable and Sustainable Energy Reviews*, 91, 1148–1161.
- NASA. (2023). NASA Prediction of Worldwide Energy Resource (POWER) database. <https://power.larc.nasa.gov/data-access-viewer/> (accessed 01.04.2023).
- Numminen, S., & Lund, P. (2019). Evaluation of the reliability of solar micro-grids in emerging markets – Issues and solutions. *Energy for Sustainable Development*, 48, 34–42.
- Ouyang, D., et al. (2020). Impact of high-temperature environment on the optimal cycle rate of lithium-ion battery. *Journal of Energy Storage*, 28, Article 101242.
- Ruggles, T. H., et al. (2020). Developing reliable hourly electricity demand data through screening and imputation. *Scientific Data*, 7, 155.
- Sayani, R., et al. (2022). Sizing solar-based mini-grids for growing electricity demand: Insights from rural India. *Journal of Physics: Energy*, 5(1).
- Seaman, S. R., Bartlett, J. W., & White, I. R. (2012). Multiple imputation of missing covariates with non-linear effects and interactions: an evaluation of statistical methods. *BMC Medical Research Methodology*, 12(1), 46.
- Seel, J., Warner, C., & Mills, A. (2020). Influence of business models on PV-battery dispatch decisions and market value: A pilot study of operating plants. *Advances in Applied Energy*, 5, Article 100076.
- Shyu, C. W. (2013). End-users' experiences with electricity supply from stand-alone mini-grid solar PV power stations in rural areas of western China. *Energy for Sustainable Development*, 17(5), 391–400.
- Wang, Z., & Perera, A. T. D. (2019). Robust optimization of power grid with distributed generation and improved reliability. *Energy Procedia*, 159, 400–405.
- Wang, Z., et al. (2017). Optimal expansion planning of isolated microgrid with renewable energy resources and controllable loads. *IET Renewable Power Generation*, 11(7), 931–940.
- Waqar, A., et al. (2015). *Optimal capacity expansion-planning of distributed generation in micro-grids considering uncertainties*. Paper presented at the 5th International Conference on Electric Utility Deregulation and Restructuring and Power Technologies (DRPT), Changsha, China. 2015 pp. 437–442.
- Warmuz, J., & De Doncker, R. W. (2019). PV- and battery-ratio for very large modular PV parks with DC coupled battery converters. In *Proceedings of the 2019 IEEE* (pp. 444–450).
- Wassie, Y. T., & Ahlgren, E. O. (2023a). Performance and reliability analysis of an off-grid PV mini-grid system in rural tropical Africa: a case study in southern Ethiopia. *Development Engineering*, 8, Article 100106.
- Wassie, Y. T., & Ahlgren, E. O. (2023b). Determinants of electricity consumption from decentralized solar PV mini-grids in rural East Africa: An econometric analysis. *Energy*, 274, Article 127351.
- Weniger, J., Tjaden, T., & Quaschnig, V. (2014). Sizing of residential PV battery systems. *Energy Procedia*, 46, 78–87.
- White, I. R., Royston, P., & Wood, A. M. (2011). Multiple imputation for chained equations: issues and guidance for practice. *Statistics in Medicine*, 30, 377–399.
- World Bank. (2023). *Solar mini-grids could sustainably power 380 million people in Africa by 2030 – If Action is taken now* (Press Release No 055, Nairobi, Kenya).
- Xie, W., et al. (2020). Challenges and opportunities toward fast-charging of lithium-ion batteries. *Journal of Energy Storage*, 32, Article 101837.

Yang, J., & Su, C. (2021). Robust optimization of microgrid based on renewable distributed power generation and load demand uncertainty. *Energy*, 223, Article 120043.

Zebra, E. I. C., et al. (2021). A review of hybrid renewable energy systems in mini-grids for off-grid electrification in developing countries. *Renewable and Sustainable Energy Reviews*, 144, Article 111036.

Zhao, Z. Y., Chen, Y. L., & Thomson, J.-D. (2017). Levelized cost of energy modeling for concentrated solar power projects: A China study. *Energy*, 120, 117–127.